LASER & PHOTONICS REVIEWS

REVIEW ARTICLE

Abstract As an emerging topic, photonic-assisted microwave measurements with distinct features such as wide frequency coverage, large instantaneous bandwidth, low frequency-dependent loss, and immunity to electromagnetic interference, have been extensively studied recently. In this article, we provide a comprehensive overview of the latest advances in photonic microwave measurements, including microwave spectrum analysis, instantaneous frequency measurement, microwave channelization, Doppler frequency-shift measurement, angle-of-arrival detection, time–frequency analysis, compressive sensing, and phase-noise measurement. A photonic microwave radar, as a functional measurement system, is also reviewed. The performance of the photonic measurement solutions is evaluated and compared with the electronic solutions. Future prospects using photonic integrated circuits and software-defined architectures to further improve the measurement performance are also discussed.
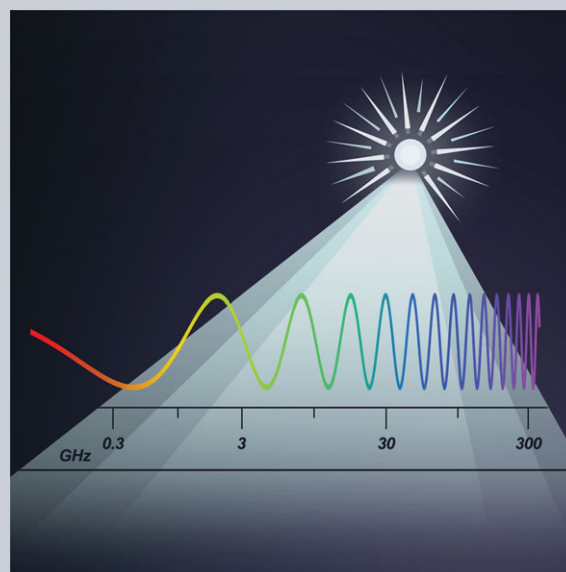
Photonics for microwave measurements

Xihua Zou[1,2,*], Bing Lu[1], Wei Pan[1], Lianshan Yan[1], Andreas Stöhr[2], and Jianping Yao[3,*]

1. Introduction

1.1. Microwave measurements

Microwave (from 300 MHz to 300 GHz [1]) theories and technologies have been extensively researched and widely applied for civil and defense applications. As one of the fundamental applications, microwave measurements are widely used in fields such as astronomy, communications, navigation, traffic and automotive control, electronic warfare, radar and warfare systems, medicine and health care, and appliances (e.g., microwave oven), as illustrated in Fig. 1. In general, the performance of microwave measurements ultimately determines the characteristics of microwave techniques and systems.

1.2. Electronic solutions and challenges

Electronic solutions are the most straightforward and still the dominant means for the implementation of microwave measurements today. Such solutions have been widely employed in microwave systems to support the realization of various traditional functionalities [2–10], such as the measurements of temporal waveform, power/voltage, frequency, spectrum, noise, scattering parameter, vector/scalar network analysis, device characterization and calibration, and remote sensing of environmental variations. In addition, a number of new functionalities have been fulfilled by electronic solutions [9], such as real-time signal analysis, multifunctional measurement, and vector network analysis for nonlinear systems.

However, due to the explosive growth of data traffic, such as high-speed wireless communications (5G and beyond), internet of things, new generation of radars, and real-time services, critical challenges are bringing urgent demands to microwave measurements in terms of large instantaneous bandwidth greater than 10 GHz and wide frequency coverage from several megahertz to hundreds of gigahertz, which may not be achievable using purely electronic solutions or the systems are extremely complicated and costly. Table 1 summarizes the performance specifications of some selected state-of-the-art real-time microwave signal analyzers. As can be seen, the maximum real-time bandwidth is limited only to ~ 500 MHz, which is far lower than the expected value of tens of gigahertz.

[1] Center for Information Photonics and Communications, School of Information Science and Technology, Southwest Jiaotong University, Chengdu, 611756, China
[2] Institute of Optoelectronics, University of Duisburg-Essen, Duisburg, 47057, Germany
[3] Microwave Photonics Research Laboratory, School of Electrical Engineering and Computer Science, University of Ottawa, Ottawa, K1N 6N5, Canada
*Corresponding authors: X. Zou, zouxihua@swjtu.edu.cn; J. Yao, jpyao@eecs.uOttawa.ca
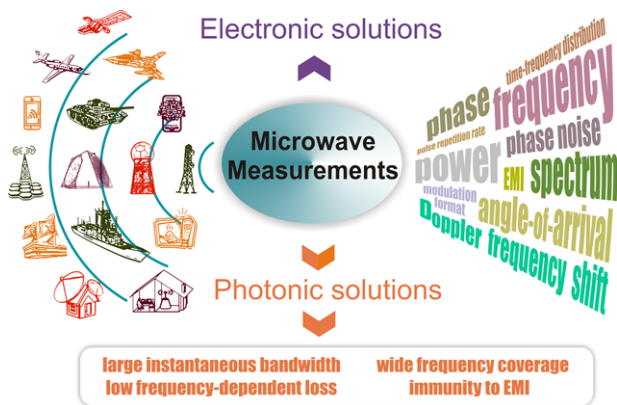
Figure 1 Microwave measurements and photonic solutions. (EMI: electromagnetic interference).

1.3. Photonics for microwave measurements

As an emerging research field, microwave photonics has been considered as an enabling technology for the generation, distribution, control, detection and measurement of microwave signals, as well as for the implementation of new devices and systems [11–27]. Among the numerous functionalities enabled by photonics, microwave measurements based on photonics can provide superior performance in terms of large instantaneous bandwidth, wide frequency coverage, low frequency-dependent loss, and

strong immunity to electromagnetic interference (EMI). Thus, photonic microwave measurement techniques have been widely researched recently and numerous new approaches have been proposed, to address the challenges facing electronic solutions.

Figure 2 illustrates a generic system architecture for photonic microwave measurements. As can be seen, the system consists of a light source, an electro-optic modulator (EOM), a photonic processing module, an optical-to-electrical (OE) conversion module, and a post processing module. The light source can be a single-wavelength continuous-wave (CW) laser, a mode-locked pulsed laser (MLL), an optical frequency comb (OFC), or a broadband light source (such as an amplified spontaneous emission source, ASE). The EOM can be an intensity, a phase, a polarization, or an electroabsorption modulator. A microwave signal with its parameters to be measured is applied to the EOM to modulate the optical carrier from the light source. The modulated optical signal carrying the microwave signal is then sent to the photonic processing module, which can be an optical comb filter, a fiber Bragg grating (FBG), an integrated resonator, or a waveguide grating filter, to perform signal processing in the optical domain. After OE conversion, the parameters of the microwave signal to be measured can be obtained in the post processing stage.

Based on this generic system architecture, numerous photonic microwave measurement techniques have been proposed. In this article, we provide a comprehensive overview of the photonic microwave measurement

Table 1 Specifications of selected state-of-the-art real-time microwave signal analyzers

| Instrument	RTSA series, Keysight	FSVR series, Rohde & Schwarz	RSA5000 series, Tektronix
Maximum real-time bandwidth	<510 MHz	40 MHz [a]	165 MHz [b]
Frequency coverage	3 Hz–26.5 GHz	10 Hz–40 GHz	1 Hz–26.5 GHz
Minimum signal duration	3.5 μs	24 μs (40-MHz span)	2.7 μs (165-MHz bandwidth)
Resolution bandwidth	287 kHz (500-MHz span)	100 kHz [c]	25 kHz (165-MHz bandwidth)
Data released	Apr. 2015	Mar. 2015	Aug. 2015

[a]Signal analysis bandwidth
[b]Real-time acquisition bandwidth or analysis bandwidth
[c]Calculated with a 40-MHz span and a span to resolution bandwidth ratio of 400.
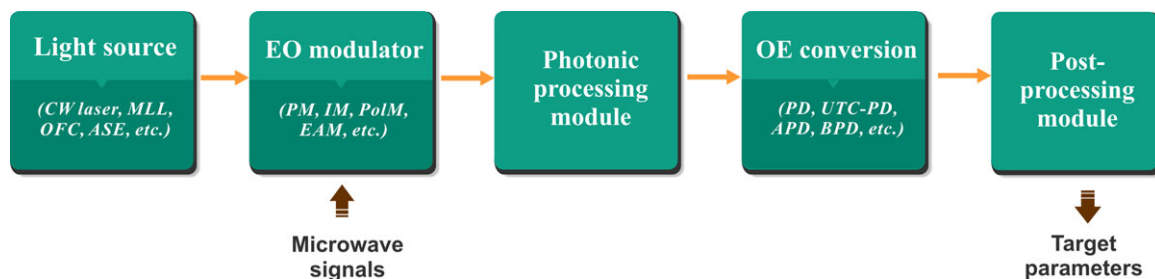
Figure 2 Generic system architecture for photonic microwave measurements. (CW: continuous-wave; MLL: mode-locked pulsed laser; OFC: optical frequency comb; ASE: amplified spontaneous emission source; EO: electro-optic; PM: phase modulator; IM: intensity modulator; PolM: polarization modulator; EAM: electroabsorption modulator; OE: optical-to-electrical; PD: photodetector; UTC-PD: uni-traveling-carrier photodiode; APD: avalanche photodiode; BPD: balanced photodetector).
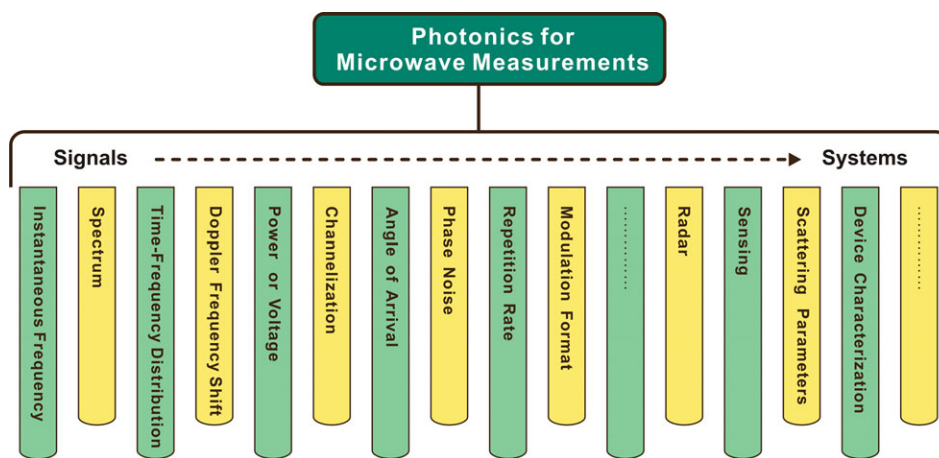
Figure 3 Measurement functionalities enabled by photonics.

techniques reported over the past few years. Different measurement functionalities, including instantaneous frequency, spectrum, time–frequency distribution, Doppler frequency shift (DFS), angle-to-arrival (AOA), and phase-noise measurements, will be presented. System applications such as ranging and sensing will also be discussed. Figure 3 summarizes the functionalities that are implemented by photonic microwave measurements.

The remainder of this article is organized as follows. From Section 2 to Section 7, recent advances in photonic microwave spectrum analysis, photonic instantaneous frequency measurement (IFM), photonics-assisted microwave channelization, photonic microwave DFS measurement, photonic AOA measurement, photonic time–frequency analysis, photonic-assisted compressive sensing and photonic phase-noise measurement, are reviewed. In Section 8, a photonic microwave radar as a functional measurement system is introduced. The results of the first field trial and the future trend towards versatile functionalities are discussed. In Section 9, the performance of the photonic measurement solutions are evaluated and compared with the electronic solutions. Future prospects using photonic integrated circuits (PICs) and software-defined architectures to further improve the measurement performance are also discussed in Section 10. In Section 11, a conclusion is drawn.

2. Microwave *spectrum analysis*

2.1. Spectrum analysis based on frequency scanning

Spectrum analysis based on frequency or wavelength scanning is a powerful tool in signal measurement in either the electrical or the optical domain. In the optical domain, for the generic system architecture shown in Fig. 2, the measurement operation is usually done by scanning the wavelength of a light source or the transmission or reflection spectral response of an optical filter. After photodetection, the microwave spectrum over a wide frequency range is recorded point by point. Basically, an optical spectrum analyzer (OSA) embedded with a scanning grating can be used to analyze the spectrum of a microwave signal by providing a wide frequency measurement range, for example, the entire C band or even C+L band, in the optical domain. In [28], an OSA was used to measure the radio-frequency (RF) spectrum of an optical signal with a record measurement range over 2.5 THz. Although the frequency measurement range is ultrawide [28], the resolution is very low due to the use of a bulky free space grating, which makes it impractical to use an OSA for microwave measurements.

To perform microwave measurements, a solution is to scan the wavelength of a light source, as shown in Fig. 2. Again, a fine tuning step should be provided to ensure a high resolution. For a laser source with a tunable wavelength, however, the wavelength stability during a fast scanning procedure is relatively poor, which would degrade the measurement accuracy. Thus, an effective solution is to use a laser source with a fixed wavelength, but the scanning is done using a fine-tuning optical filter. Typically, the optical filter used for scanning can be a Fabry–Pérot etalon, an echelle diffractive grating (EDG), an FBG or a tunable photonic microwave filter [29–32]. In [29], a scanning receiver in which the scanning was performed using a Fabry–Pérot etalon was demonstrated, providing a frequency measurement range of 40 GHz and a resolution of 90 MHz. In [30], an electrically tunable FBG with a 54-MHz transmission bandwidth having steep slopes was utilized to analyze the spectrum of a microwave signal, providing a frequency measurement range of 7 GHz, from 2 to 9 GHz. In [31], a monolithically integrated EDG having 15 channels was employed to measure the spectrum of a microwave signal. A resolution of 50 MHz was obtained for a frequency measurement range from 0 to 15 GHz when monotonically scanning the wavelength of a channel. If all the 15 channels are used, the overall measurement range can be 225 GHz. In [32], a two-tap tunable photonic microwave filter using two laser sources was employed for spectrum analysis. When the wavelength of one laser source was tuned, a spectral response with different free spectral ranges (FSRs) was generated after photodetection. Multiple microwave powers for different FSRs were collected to form an interferogram
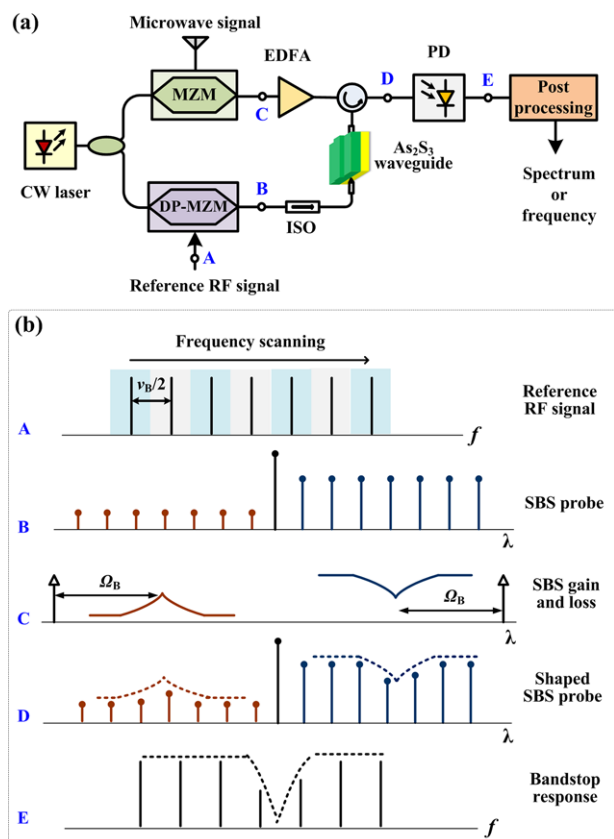
Figure 4 Spectrum analysis system based on a scanning receiver using a chip-based photonic Brillouin filter: (a) experimental setup and (b) the optical/RF spectra measured at different points A–E [37]. (LD, laser; OC, optical coupler; MZM, Mach–Zehnder modulator; DP-MZM, dual-parallel MZM; EDFA, erbium-doped fiber amplifier; ISO, isolator; PD, photodetector; v_B, Brillouin linewidth; Ω_B, SBS frequency shift).
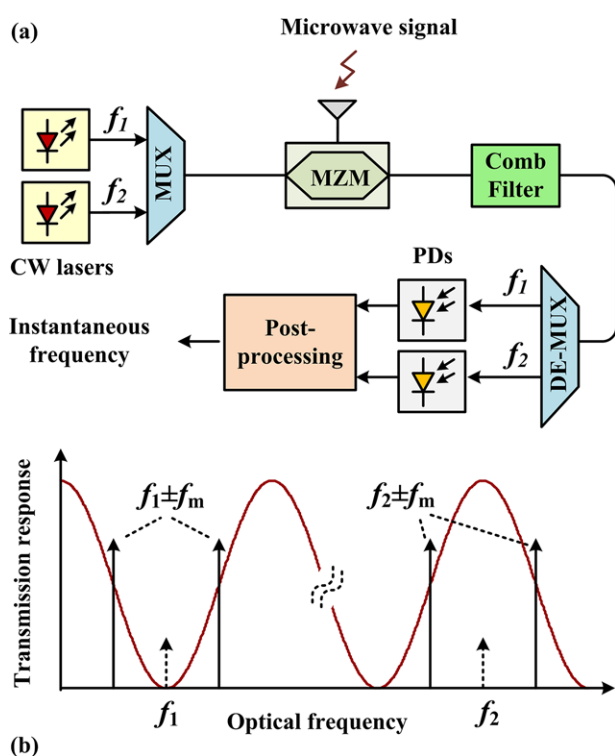
2.2. Featured example

Very recently, a photonic frequency-scanning receiver using a chip-based photonic Brillouin filter was proposed for microwave spectrum analysis. The schematic diagram is illustrated in Fig. 4 [37]. In one path, an RF reference signal with its frequency scanning at a fixed step of 25 MHz is fed into a dual parallel Mach–Zehnder modulator (DP-MZM). A phase-modulated signal is generated, which is used as a probe signal and sent to an achalgogenite (As_2S_3) rib waveguide where the SBS will be triggered when a pump signal is injected into the As_2S_3 waveguide from the opposite direction. Note that for this phase-modulated optical signal, the two optical sidebands are with unequal amplitudes but out of phase. In the other path, a microwave signal is applied to an MZM that is biased at the minimum transmission point for carrier suppression, providing two first-order optical sidebands. The two optical sidebands are amplified by an erbium-doped fiber amplifier (EDFA) and then injected into the nonlinear As_2S_3 waveguide as an SBS pump. An SBS gain and an SBS loss spectra are simultaneously generated. A bandstop filter is then formed because of the amplitude balance caused by the SBS gain and loss, such that the output microwave power is monitored to reveal the microwave frequency based on the frequency-to-power mapping. A division between the two output microwave powers measured at two adjacent frequency points of the reference RF signal when its frequency is scanning at a step of 25 MHz, is performed to derive a large-slope amplitude comparison function. Thus, the microwave spectrum was measured by detecting the frequency information step by step, wherein a coarse estimation was first performed by scanning the RF reference signal and a high-precision measurement was then implemented through the frequency-to-power mapping. In the experiment, a frequency measurement range from 9 to 38 GHz was demonstrated with a measurement error less than 1 MHz [37], thanks to the combination of the frequency agility of a scanning receiver and the large slope of the amplitude comparison function.

Compared with an electrical scanning receiver or an electrical spectrum analyzer, this photonic solution is able to circumvent the trade-off between the accuracy and the acquisition time for a wide frequency measurement range. A 1-MHz resolution for a frequency scanning step of 25 MHz was obtained in tens of nanoseconds due to the large slope of the amplitude comparison function. In an electrical spectrum analyzer, for the same resolution a frequency scanning step of only $\sim$1 MHz can be performed. Thus, the use of this photonic solution can greatly reduce the overall measurement time [37].

3. Instantaneous frequency measurement

The photonic microwave measurement techniques based on frequency scanning are able to analyze the spectrum of a periodic signal or an aperiodic signal with a long time duration, but are unable to capture the instantaneous frequency

that was then processed by fast Fourier transform (FFT) to perform microwave spectrum analysis. A fine resolution of 15 MHz was demonstrated [32].

In addition to the use of a tunable optical filter, a stimulated Brillouin scattering (SBS) gain or loss spectrum having an ultranarrow bandwidth can also be used to perform microwave spectrum analysis [33–36]. In general, the bandwidth of the SBS gain or loss spectrum is about 20 MHz, thus it can be utilized to perform microwave frequency analysis with a resolution of 20 MHz [33]. To further increase the resolution, one may superimpose an SBS gain spectrum with two loss spectra to reduce the bandwidth of the SBS gain. It was reported in [34] that a reduced bandwidth from 20 to $\sim$3.4 MHz was achieved. Another solution to increase the resolution is to use a polarization pulling assisted SBS and heterodyning detection. For instance, a measurement resolution as high as 1 kHz was demonstrated [35, 36].
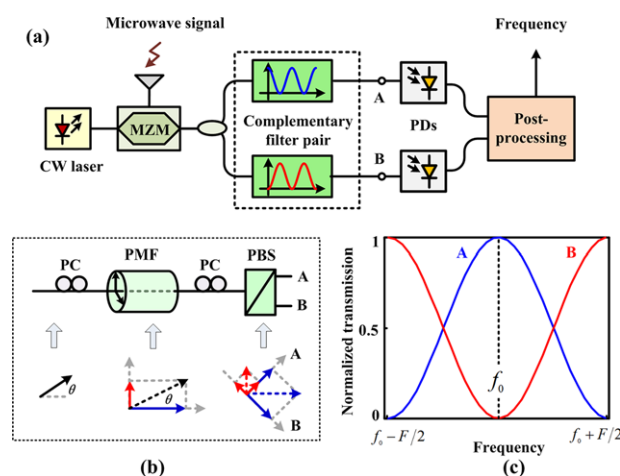
Figure 5 (a) Schematic diagram and (b) the operation principle of a photonic IFM system based on an optical comb filter.(CW: continuous wave; MUX: multiplexer; MZM: Mach–Zehnder modulator; DE-MUX: demultiplexer; PD: photodetector).
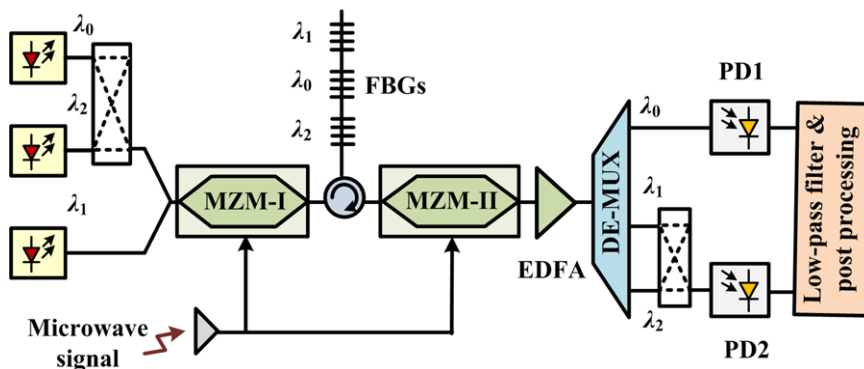

Figure 6 Photonic IFM system based on a complementary comb filter pair: (a) schematic diagram of the system, (b) the complementary filter pair, and (c) the spectral responses of the complementary filter pair. (CW: continuous wave; MZM: Mach–Zehnder modulator; PD: photodetector; PC: polarization controller; PMF: polarization maintaining fiber; PBS: polarization beam splitter).

of an abrupt or a frequency-agile microwave signal. IFM is of critical importance for various applications such as radar, electronic warfare and cognitive radio. Accordingly, numerous photonic approaches have been proposed recently. In general, photonic IFM can be realized by mapping the frequency information to an optical or microwave power. The power information can be measured instantaneously and thus IFM can be realized. The frequency-to-power mapping can be implemented using an optical comb filter, an optical mixing unit, or a dispersive delay element.

3.1. Based on an optical comb filter

By utilizing an optical comb filter, the instantaneous frequency of a microwave signal can be converted to an optical power through frequency-to-power mapping [38–52]. By detecting the optical power, the instantaneous frequency can be measured. Figure 5a illustrates such a photonic IFM system using an optical comb filter [38]. A microwave signal is received and applied to an MZM to modulate two optical carriers at f_1 and f_2. The MZM is biased at the minimum transmission point to achieve a carrier-suppressed double sideband (CS-DSB) modulation. Then, the modulated optical signals are sent to an optical comb filter that has a sinusoidal spectral response. The wavelength of one optical carrier is aligned with one peak of the comb response

and the wavelength of the other carrier is aligned with one valley of the comb response, as shown in Fig. 5b. The two optical signals are de-multiplexed and then sent to two photodetectors (PDs). Two optical powers are measured at the output of the PDs and a power ratio between them is a function of the microwave frequency. Thus, by monitoring the power ratio, the instantaneous frequency of a microwave signal is measured. The approach was verified by an experiment [38]. A frequency measurement range of 1–20 GHz and a measurement error below ±200 MHz were achieved when using a comb filter (i.e., a Sagnac loop) with an FSR of 50 GHz. The measurement error was mainly caused by the bias drift of the MZM and the wavelength drift of the two laser sources.

The photonic approach in [38] could be simplified by removing the second laser source when using a complementary optical comb filter pair [39–45]. Figure 6 shows the schematic diagram of such a photonic IFM system based on a complementary comb filter pair. The filter pair was implemented by employing a length of polarization-maintaining fiber (PMF) in conjunction with a polarization beam splitter (PBS) [39]. Thanks to the two complementary spectral responses, as shown in Fig. 6c, two frequency-dependent optical powers are detected and the power ratio (R) between them is given by

$$R = \frac{1 - r\cos(2\pi f_{\mathrm{m}}/F)}{1 + r\cos(2\pi f_{\mathrm{m}}/F)}, \qquad (1)$$

where F denotes the FSR of the comb filter, f_{m} is the instantaneous frequency of the microwave signal, and r is the relative peak-to-notch contrast ratio of the two complementary transmission responses. As can be seen from Eq. (1), the instantaneous frequency is independent of microwave power, and can be estimated from the power ratio within the

Figure 7 Block diagram of the photonic IFM system based on an optical mixing unit with two orthogonal outputs. (MZM: Mach–Zehnder modulator; FBG: fiber Bragg grating; EDFA: erbium-doped fiber amplifier; DE-MUX: demultiplexer; PD: photodetector).

frequency measurement range of half the FSR. The approch was verified by an experiment, showing a measurement error less than ±200 MHz for a frequency measurement range of 25 GHz from 1 to 26 GHz.

By replacing the complementary comb pair with two quadrature comb filters, the frequency measurement range can be further increased from half FSR to a full FSR [42, 43].

In addition to the measurement of the instantaneous frequency of a microwave signal, the photonic IFM system using a comb filter can also be used to measure other parameters of a pulsed microwave signal. In [44], it was reported that other parameters including the signal amplitude, time duration, and time of arrive (TOA), could also be measured in addition to the instantaneous frequency. The measurement errors were estimated to be less than ±100 MHz, ±0.05 V, ±1 ns, and ±0.16 ns within a frequency range from 2 to 11 GHz for the instantaneous frequency, amplitude, time duration, and TOA, respectively.

The approaches reported in [38–44] can achieve IFM for both a pulsed and a CW microwave signal, but are unable to discriminate the two types of signals. Recently, a photonic approach capable of performing both IFM and signal classification was proposed [45]. After the frequency-to-power mapping implemented by two optical complementary filters, either a low-frequency alternating currency (AC) or a direct current (DC) electrical component that is frequency dependent can be generated for a pulsed or a CW microwave signal. The frequency of a pulsed microwave signal is estimated from the AC component, while the frequency of a CW signal is measured from the DC component. A successful discrimination between a CW and a pulsed microwave signal can be achieved. The frequency measurement error was estimated to be less than ±80 MHz and ±100 MHz for a CW and a pulsed signal, respectively, for a frequency measurement range from 5 to 20 GHz.

The optical comb filters in [38–45] were implemented using discrete fiber-optic components. To improve the operation stability, integrated optical comb filters are highly desired for performing IFM [46–50]. For example, a monolithically integrated ring-assisted Mach–Zehnder interferometer with two complementary comb spectral responses was employed to measure the instantaneous frequency of a microwave signal. The root mean square (RMS) error was estimated to be less than 200 MHz for a frequency measurement range between 5 and 15 GHz [50].

On the other hand, an FBG with two complementary slopes in its spectral response could also be used in a photonic IFM system to ensure a good stability [51, 52].

3.2. Based on an optical mixing unit

Optical mixing is another significant way to perform photonic IFM. A mixing between an optical signal modulated by a microwave signal and its replica with a given time delay could give rise to an optical power that is dependent of the microwave frequency. Thus, the IFM is realized by detecting the output power at the output of an optical mixing unit that can be implemented using two cascaded modulators [53, 54] or based on optical nonlinear effect such as four-wave mixing (FWM) [55–59]. In [53], a received microwave signal was equally divided into two parts and applied to two cascaded MZMs, to perform optical mixing. An unambiguous frequency measurement range from 2.2 to 3 GHz was experimentally demonstrated. The small frequency measurement range was limited by the frequency-dependent transmission loss and the long time delay of the coaxial cable used in the experiment. To increase the unambiguous frequency measurement range, a small time delay can be introduced from an optical link to avoid the distortions arising from a coaxial cable. In [54], a photonic system consisting of three laser sources and three FBGs were adopted to obtain a small time delay. As depicted in Fig. 7, the three FBGs centered at λ_0, λ_1 and λ_2 are connected in series to construct a two-tap transversal microwave filter with a reference tap at λ_0. A frequency-independent, lower time delay between λ_1 and λ_2 is obtained and hence the frequency measurement range can be extended up to 10 GHz.

Optical mixing can also be carried out through FWM within a highly nonlinear fiber (HNLF) [55–59]. By detecting the power of the idler component arising from the FWM effect, the microwave instantaneous frequency can be effectively estimated inside multiple unambiguous, piecewise frequency bands, which can be combined together to offer a wide frequency measurement range up to 40 GHz [56].
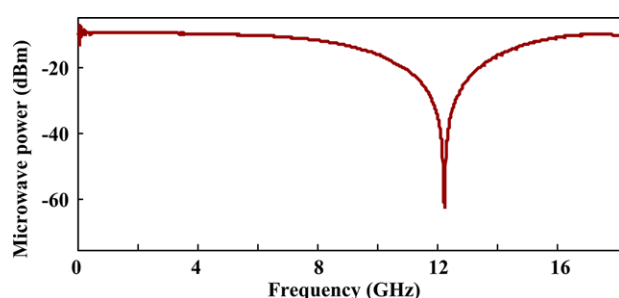
Figure 8 Measured microwave power fading arising from chromatic dispersion.

3.3. Based on a dispersive delay element

The IFM approaches can be developed by introducing a dispersive delay element that is used to generate a dispersion-induced microwave power fading [60–71] or to design a photonic microwave filter [72–77]. Since both the microwave power fading and the spectral response of a microwave filter are frequency dependent, the instantaneous frequency of a microwave signal is measured by detecting the microwave power.

As is known, an optical double sideband signal would suffer from a frequency-dependent power fading caused by the chromatic dispersion of an optical link [78]. Figure 8 shows the power fading for an optical double sideband signal traveling in a 24.6-km single mode fiber. It can be seen within a specific frequency range, the detected microwave power has a monotonic relationship with the instantaneous frequency without ambiguity.

To make the frequency measurement independent of the microwave power, two or more frequency-dependent powers in two or more channels are detected and then employed to derive one or more power ratios, which are microwave power independent. For example, if two channels are employed, two frequency-dependent powers can be detected and the ratio between them is given by

$$R = \frac{P_1}{P_2} = \frac{\Re_1 \cos^2\left(\pi \chi_1 \lambda_1 f_\mathrm{m}^2/c + \alpha\right)}{\Re_2 \cos^2\left(\pi \chi_2 \lambda_2 f_\mathrm{m}^2/c + \beta\right)}, \qquad (2)$$

where c is the light velocity in vacuum, λ_1 and λ_2 denote the wavelengths of the two channels. P_1 and P_2, $\Re_1$ and $\Re_2$, χ_1 and χ_2 are the detected microwave powers, the link losses, and the chromatic dispersions at the two channels, respectively. Here, it is worth highlighting that the phase shifts (α and β) of the two channels can be flexibly optimized using intensity, phase or polarization modulation or an SBS-based signal processing module [60–71], allowing a fully tunable frequency measurement range and an adjustable resolution.

While in an electronic IFM receiver, the microwave instantaneous frequency is measured by a number of interferometric phase discriminators based on multiple delay lines with different physical lengths [6, 79]. In such a receiver, the longest delay line determines the resolution, whereas

the shortest one guarantees a wide unambiguous frequency measurement range [80]. For this reason, an electronic IFM receiver is able to achieve a fine resolution of a few megahertz in a frequency measurement range of a few to tens of gigahertz [81, 82]. As an example, an electronic frequency measurement unit (DR058-F1 from Teledyne Defense [82]) is able to intercept a microwave signal with a frequency range from 2 and 18 GHz, offering a nominal resolution of 1 MHz.

4. Photonic-assisted microwave channelization

A microwave channelizer is a device that is able to slice the spectrum of a microwave signal into a bank of narrow channels and each channel provides a high-resolution and high-sensitivity measurement for a channel bandwidth in this channel. Currently, photonic-assisted microwave channelizers have been developed based on space-division multiplexing (SDM) [83,84], wavelength-division multiplexing (WDM) [85–99], and time-division multiplexing (TDM) [100–103].
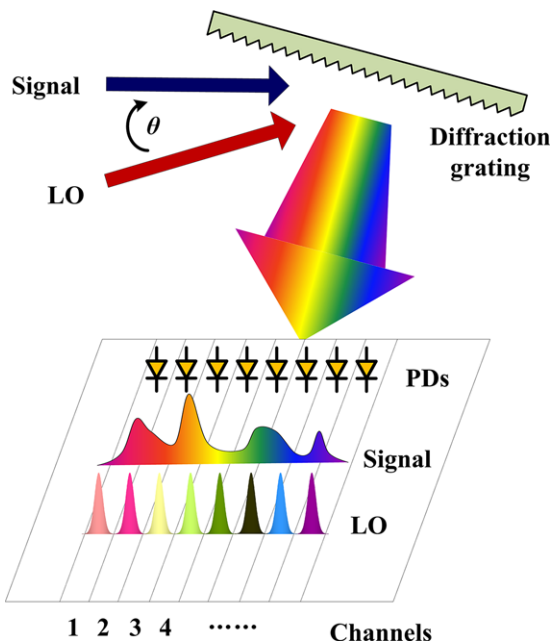
4.1. Based on space-division multiplexing

Based on SDM, the frequency components of a microwave signal are spatially dispersed in the optical domain, to have multiple parallel and spatially separated channels. At each spatial channel, only a microwave signal falling inside a specific frequency band can be measured at a high resolution. Such photonic microwave channelizers can be implemented by using a free-space diffraction grating [83], an integrated optical hybrid Fresnel lens system [84], or an acoustic-optic component, to provide angular dispersion.

Figure 9 shows a photonic-assisted microwave channelizer using a free-space diffraction grating [83]. Different frequency components of the microwave signal modulated on an optical carrier are spatially dispersed and subsequently separated in space. An OFC serving as a local oscillator (LO) beam is injected with a spatial offset to the diffraction grating, to ensure a constant frequency difference or fixed intermediate frequency (IF) between the spatially overlapping signal beam and the LO beam for performing frequency downconversion. An array of PDs is utilized to identify the spatially separated frequency components and each PD covers a specific frequency band or channel. An experiment was performed and all channels were operating at a nominal 5-GHz IF band and offering a channel resolution of 1 GHz [83], which would yield a total instantaneous bandwidth greater than 100 GHz.

4.2. Based on wavelength-division multiplexing

Based on WDM, the frequency components of a microwave signal are spectrally sliced in the optical domain, to have

LASER
& PHOTONICS
REVIEWS

Figure 9 Microwave channelizer based on space-division multiplexing using a free-space diffraction grating. (PD: photodetector; LO: local oscillator).

Figure 10 (a) Microwave channelizer using a spectrally sliced incoherent source and two Fabry–Pérot etalons; (b) spectral responses of two etalons. (ILS: incoherent light source; EOM: electro-optic modulator; DE-MUX: demultiplexer; PD: photodetector; FSR: free spectral range).

multiple parallel and spectrally separated channels. At each wavelength channel, only a specific frequency band can be processed at a high resolution. In such a system, a microwave signal is applied to modulate the light wave from an ASE source, a tunable laser source, a laser array, or an OFC, with the spectrum of a microwave signal being multicasted into a host of wavelength channels with a regular ITU-T channel spacing (e.g., 0.4 or 0.8 nm). By using an optical comb filter with a high fineness or a filter array with a narrow bandwidth, only a small band of the microwave spectrum is recorded at a wavelength channel. A WDM demultiplexer is then used to separate the wavelength channels and each channel covers a specific, small band of the spectrum of the microwave signal, resulting in a high channel resolution.

A photonic-assisted channelizer can be implemented using an array of EO waveguide delay lines [85], an array of phase-shifted FBGs [86], an integrated optical micro-ring resonator [87], a Fabry–Pérot etalon, or an OFC combined with a WDM demultiplexer [88–94].

Figure 10 shows, for instance, a photonic-assisted channelizer consisting of a spectrally sliced incoherent source and two Fabry–Pérot etalons (Etalon-I and Etalon-II) [89]. Here, Etalon-I is employed to carve the broadband incoherent light source into a multiwavelength carrier to be used for the spectrum multicast. A microwave signal to be measured is applied to an EOM to produce a double sideband modulation at the multiple wavelengths, and Etalon-II is used to select the optical sidebands after EO modulation. As a difference (say X GHz) is set between the FSRs (i.e., FSR_1 and FSR_2) of the two etalons, each channel of Etalon-II covers a specific frequency band of the microwave spectrum,
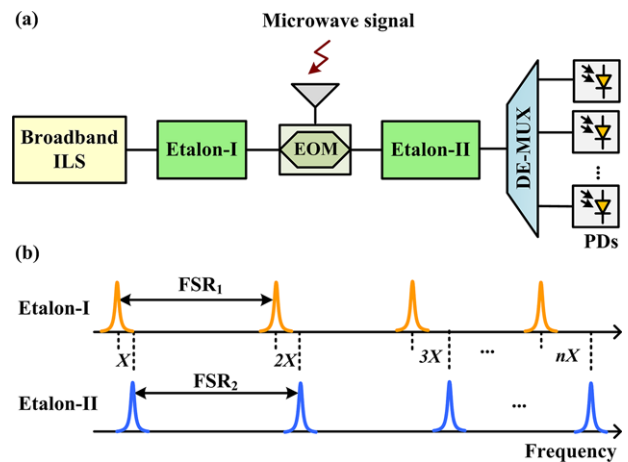
as shown in Fig. 10b. A WDM demultiplexer is then connected after Etalon-II to de-multiplex the multiple channels from Etalon-II. Microwave channelization with a channel resolution of X GHz is thus realized. The same approach was also implemented by replacing the sliced incoherent light source with an OFC, to improve the signal quality at the output of the demultiplexer and the tuning operation of the system [90–94]. For the channelizers reported in [89–94], the channel resolution was mostly estimated to be ± 2.5 GHz or ± 0.5 GHz, which was limited by the bandwidth of the used optical etalons or filters.

To enhance the channel resolution, from a few gigahertz to tens of megahertz or even tens of kilohertz, channelizers based on an OFC in conjunction with an inphase and quadrature (IQ) demodulator [95] or an SBS processing unit [96, 97], have been proposed. Figure 11a shows the schematic diagram of the channelizer using an SBS processing unit [96]. The configuration has two parallel paths. In the upper path, multiple optical carriers are modulated by a microwave signal to be measured. In the lower path, each optical carrier is frequency shifted and spectrum shaped to have a rectangular profile, which are then utilized to pump a SBS element via an optical circulator to produce multiple gain channels, with each channel having a narrow and rectangular profile. A WDM demultiplexer is connected after the optical circulator to separate the multiple modulated optical carriers. Consequently, an array of microwave channels is realized with a channel resolution identical to the bandwidth of the SBS gain, as shown in Fig. 10b. In addition to an improved channel resolution, the channelizer can be controlled to have a tunable bandwidth, channel spacing and channel profile. The approach was verified by using an experimental setup shown in Fig. 11c. The results showed that the channelizer provided a shape factor less than 2, a tunable channel bandwidth from 40 to 90 MHz, and a programmable channel spacing from 50 to 80 MHz.
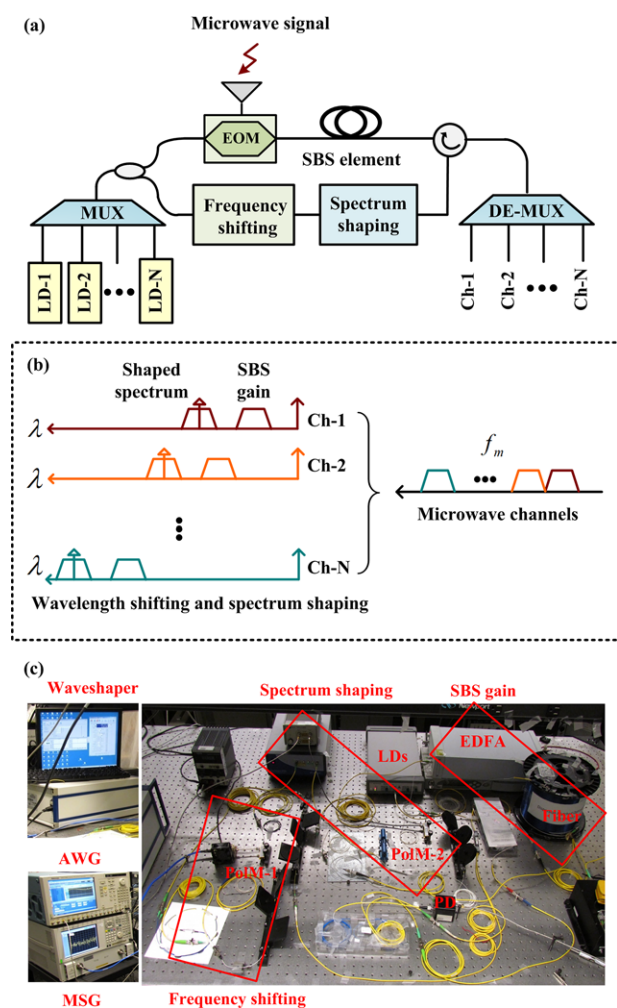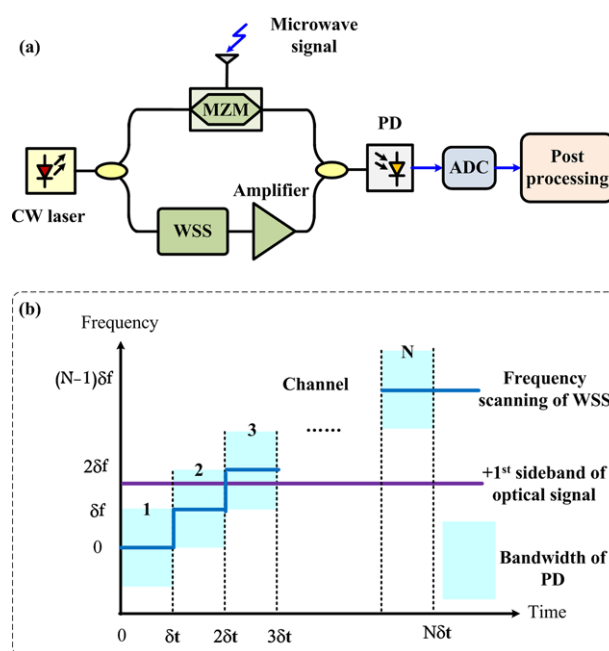
Figure 11 Photonic-assisted microwave channelizer using a SBS processing unit: (a) schematic diagram, (b) operation principle, and (c) experimental setup. (LD: laser diode; MUX: multiplexer; EOM: electro-optic modulator; SBS: stimulated Brillouin scattering; DE-MUX: demultiplexer; Ch: channel; PolM: polarization modulator; EDFA: erbium-doped fiber amplifier; MSG: microwave signal generator; AWG: arbitrary waveform generator; PD: photodetector).

Figure 12 Microwave channelizer based on time-division multiplexing using a wavelength-scanning source: (a) schematic diagram and (b) operation principle. (MZM: Mach–Zehnder modulator; WSS: wavelength scanning source; PD: photodetector; ADC: analog-to-digital conversion).

Under some stringent conditions, a much higher channel resolution can be obtained by using the spatial-spectral (S2) material. In [98], rare-earth dopant ions were doped into the S2 crystal and equivalently considered as a bank of narrow filters to perform microwave channelization. A resolution as high as ~25 kHz was achieved at the cryogenic temperature of 4–6 K, due to the narrow optical resonances of the doped rare-earth ions at ultralow temperature.

4.3. Based on time-division multiplexing

Based on TDM, the spectrum of a microwave signal to be measured is mapped into the temporal domain by using an optical wavelength scanning source (WSS) or a fre-

quency shifting recirculating loop [100–103], to generate multiple temporally separated time slots in series. By analyzing the time slots of the obtained temporal waveform, a TDM-based microwave channelizer can be realized at a high resolution.

Taking the microwave channelizer reported in [100] as an example, it was implemented using an optical WSS. As illustrated in Fig. 12a, the channelizer is comprised of two paths. In the upper path, a microwave signal is applied to an MZM. In the lower path, a WSS with a high scanning speed is utilized to linearly shift the wavelength of the optical carrier at a given wavelength step. The two optical signals from the two paths are combined and coupled to a low-bandwidth PD for performing heterodyning detection. As shown in Fig. 12b, only the beating component generated from heterodyning detection falling inside the bandwidth of the PD can be measured such that each scanning wavelength indicates a certain microwave band. Inside a scanning period of the WSS, the spectrum of the microwave signal is temporally sliced and allocated into a bank of time slots by incorporating heterodyning detection and wavelength scanning. Within a scanning period of 5 μs, a 2-MHz resolution was experimentally achieved for the measurement of a multiple-tone or a frequency-chirped signal in a 20-GHz frequency range.

Other solutions based on TDM can be implemented using coherent detection [101] or Nyquist-bandwidth detection [102]. To extend the frequency measurement range, in [103] a frequency-to-time mapping approach based on successively frequency shifting the modulation sideband of an

optical signal was proposed to perform TDM-based spectrum measurements. A readily extended frequency measurement range to 100 GHz can be achieved for the channelizer, while retaining a channel resolution of 250 MHz.

The advantage of using photonics to perform microwave channelization is the wideband frequency measurement range. An electronic channelizer, on the other hand, can provide better channel resolution. In general, an electronic channelizer is usually implemented using an analog, digital or hybrid filter bank [2, 104–107]. The use of a hybrid filter bank is attractive because of a simplified hardware implementation and an improved channel resolution. Taking the bioinspired hybrid filter bank reported in [107] as an example, an 8-channel RF filter with a channel bandwidth of 50 MHz was designed to slice the signal spectrum into 8 bands. Each band was further sliced into 8 parallel channels at the IF channelization stage. In total, 64 channels were formed for the channelized receiver, which had a channel resolution of 6.25 MHz but a frequency measurement range of only 400 MHz from 1.3 to 1.7 GHz.

## 5. Microwave Doppler frequency-shift measurement

The DFS measurement plays a critical role in many applications, such as mobile communications, metrology, medical imaging, electronic warfare, and radar systems [2, 4, 5, 7, 108–111]. Recently, several photonic approaches based on optical mixing or optical vector mixing were proposed to perform DFS measurement [112–114], with a wider frequency coverage or frequency tuning range, as compared with conventional electronic solutions.

5.1. Based on photonic mixing

Due to a frequency shift caused by the Doppler effect, the mixing between a transmitted microwave signal and its echo signal in the optical domain would yield a low-frequency electrical signal. The DFS can be obtained by analyzing the low-frequency electrical signal.

Such a photonic approach based on optical mixing was proposed by using two cascaded EOMs [112]. As shown in Fig. 13, a replica of the transmitted microwave signal is applied to an EOM (EOM-I) biased at the minimum transmission point to modulate the optical carrier. The received echo signal is applied to a second EOM (EOM-II) to modulate the optical signal from EOM-I. Two optical sidebands close to the optical carrier are generated at the output of EOM-II and then applied to a low-speed PD where a low-frequency electrical signal could be detected. Mathematically, the low-frequency electrical signal with a frequency of Δf is generated and the corresponding DFS (f_D) is given by

$$f_D = \Delta f/2 = \left| f_m - f_m' \right|/2, \qquad (3)$$
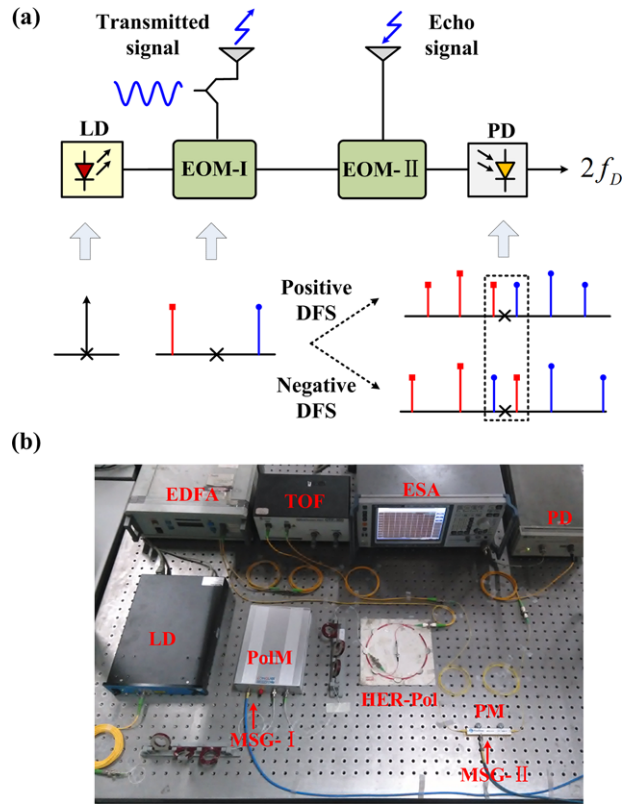
Figure 13 Photonic DFS measurement system based on optical mixing: (a) schematic diagram and (b) experimental setup [112]. (LD: laser diode; EOM: electro-optic modulator; PD: photodetector; EDFA: erbium-doped fiber amplifier; TOF: tunable optical filter; PolM: polarization modulator; HER-Pol: high extinction ratio polarizer; MSG: microwave signal generator; PM: phase modulator; ESA: electrical spectrum analyzer).

where f_m and f_m' are the frequencies of the transmitted microwave and the echo signals. Consequently, the DFS can be obtained through frequency analysis of this low-frequency electrical signal. From Eq. (3), we can see that the resolution is improved by a factor of 2. According to the measured DFS, for a monostatic radar with the transmitter and the receiver installed at the same location, the corresponding radial velocity of relative motion can be calculated by

$$v = \frac{f_D}{2f_m}c = \frac{\Delta f}{4f_m}c \qquad (4)$$

where v is the radial velocity of relative motion. The DFS was experimentally measured at different frequency bands of 10, 15 and 30 GHz in [112]. In all these cases, a measurement error was estimated to be less than 1×10^{-9} Hz within a frequency shift range from –90 to +90 kHz. However, this approach is unlikely to discriminate the direction of the DFS independently. To eliminate the direction ambiguity, a reference branch should be added.
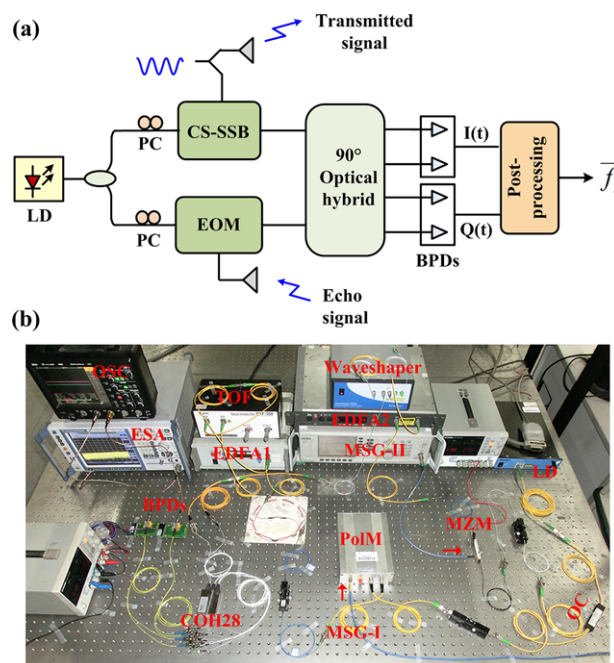
5.2. Based on optical vector mixing

For many applications it is essential to detect the DFS as well as the direction. To meet this requirement, the optical vector mixing, which is the combination of an optical frequency offset and a conventional optical mixing, can be used.

In [113], a photonic DFS measurement system was designed with two paths. In one path, the optical carrier is upshifted by a specific offset of ∼200 MHz using an optical frequency shift module (e.g., an acousto-optic modulator). This frequency offset acts as a reference to discriminate a negative DFS from a positive one. In the other path, the optical carrier is modulated by a microwave echo signal. Then, the optical signals from the two paths are combined and coupled into a low-speed PD to generate a low-frequency electrical signal. By subtracting the frequency of the generated low-frequency signal from the frequency offset, both the direction (i.e., + or −) and the DFS value (i.e., absolute value) can be obtained. In the experiments, the measurement error was estimated to be less than ±60 Hz within a DFS measurement range from –90 to +90 kHz, for carrier frequencies at 10, 15, and 20 GHz.

In [114], an enhanced photonic approach based on optical vector mixing was proposed in which an IQ coherent detection was employed. As shown in Fig. 14a, the IQ detector consists of an optical hybrid and two balanced photodetectors (BPDs), of which at the output two low-frequency electrical signals can be detected, $I(t)$ and $Q(t)$. The sign of the DFS can be determined by differentiating the phase relationship between $I(t)$ and $Q(t)$. When $Q(t)$ is delayed by $\pi/2$ with respect to $I(t)$, a positive direction is derived. Otherwise, if $Q(t)$ is $\pi/2$ advanced with respect to $I(t)$, a negative sign is obtained. Thus, the microwave DFS can be measured with a greatly improved resolution and an unambiguous direction. Within the carrier frequency range from 10 to 38 GHz, the photonic approach was experimentally validated with a measurement error less than ±5.8 Hz within a DFS range from –90 to +90 kHz, which was one order of magnitude lower than that (i.e., ±60 Hz) reported in [113]. The resolution of the radial velocity measurement was also improved by one order of magnitude.

Electronic Doppler radars operating in CW or pulse mode have already been used for velocity and distance detection through frequency shift or offset estimation. Such radars can operate at different frequency bands such as 10, 24, 35, 94 or 100 GHz, with a tunable frequency range from several MHz to 9 GHz [7, 109–111]. For example, a compact 94-GHz radar and a low-cost 100-GHz frequency-modulated radar were developed for high-resolution sensing, showing a frequency tuning range of 6 GHz [110] and 9 GHz [111]. Meanwhile, a DFS of 926 Hz was estimated for detecting a target moving at 5 km h^{-1}. Compared with electronic Doppler radars, the operation of the photonic-assisted systems [112–114] is independent of the frequency of the microwave carrier in theory. It was also experimentally demonstrated that these systems can provide a wider frequency coverage from 10 to 38 GHz.

Figure 14 Photonic DFS measurement system based on optical vector mixing: (a) schematic diagram and (b) experimental setup. (LD; laser diode; PC: polarization controller; CS-SSB: carrier-suppressed single-sideband modulation; EOM: electro-optic modulator; BPD: balanced photodetector; I: inphase; Q: quadrature; OC: optical coupler; MZM: Mach–Zehnder modulator; PolM: polarization modulator; MSG: microwave signal generator; EDFA: erbium-doped fiber amplifier; TOF: tunable optical filter; ESA; electrical spectrum analyzer; OSC: oscilloscope; $\bar{f}_{\rm D}$, Doppler frequency shift with positive or negative direction).

6. Photonic measurement of angle-of-arrival

The AOA is an important parameter used to determine the propagation direction of a microwave signal and hence the location or position of a microwave transmitter or source in civil and defense applications. Generally, the AOA can be measured under two different circumstances, the far field and the near field.

6.1. Far-field AOA measurement

In the far-field scenario, the distance between the source and the measurement system is long and the microwave signal to be measured would reach all receivers or array antenna elements in parallel or in the same direction. The AOA can be measured by detecting the delays among receiving units or array antenna elements for an incident microwave signal.

A host of photonic approaches have been proposed and experimentally demonstrated [115–122]. In [115], a simple approach using a two-tap transversal photonic microwave filter was proposed to measure the AOA. The two taps of
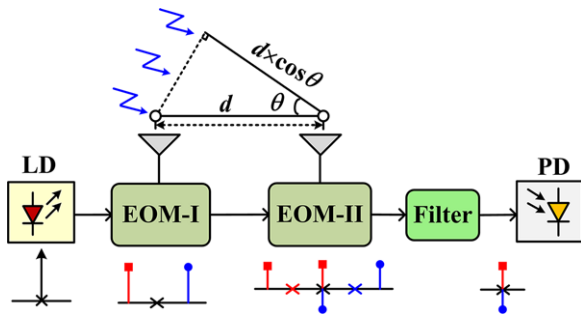
Figure 15 Schematic diagram of a photonic AOA measurement system. (LD: laser diode; EOM: electro-optic modulator; PD: photodetector).

the filter are realized by using two MZMs with a time delay between the two taps. The AOA is then estimated from the transmission notches of this filter. In [116], a photonic approach to estimate the AOA of a microwave signal using two cascaded EOMs (EOM-I and EOM-II) was proposed. As shown in Fig. 15, the two EOMs are biased at the minimum transmission point to suppress the optical carrier. When an incoming microwave signal is received and sent to the two EOMs, a new optical component located at the wavelength of the optical carrier is generated, which is the sum of one +1st- and one −1st-order sidebands of the optical signals generated from the cascade of EOM-I and EOM-II. The total power of the new optical component is a function of the AOA, due to constructive or destructive interference resulting from AOA. Thus, detecting the optical power at the carrier wavelength reveals both the AOA and the time difference of arrival (TDOA). Mathematically, the AOA (i.e., θ) is given by

$$\theta = \cos^{-1}(\tau c/d), \qquad (5)$$

where τ is the TDOA which is proportional to d, the distance between the two antenna elements connected to the two EOMs. The two EOMs in the system in [116] could be replaced by a single dual-electrode MZM [117] or DP-MZM [118], for implementing DFS measurement. An array of integrated optical ring resonators (ORR) was employed for AOA or radiation pattern measurement in [119], providing an instantaneous bandwidth of 500 MHz or wider.

The photonic AOA measurement can be facilitated by advanced system theories or intelligent algorithms, such as the robust symmetrical number system (RSNS) [120], the neuronal algorithm [121], and the correlative spectrum analysis [122]. Assisted by a photonic RSNS technique, a system to achieve unambiguous AOA measurement was demonstrated with a finer spatial resolution and a smaller array size, than using a conventional linear array. The neurobiological learning algorithm (spike timing dependent plasticity, STDP) realized by cooperatively using the cross-gain modulation (XGM) and the nonlinear polarization rotation in a semiconductor optical amplifier also powered the AOA measurement and the three-dimensional (3D) localization with an accuracy of tens of centimeters [121].

Another photonic AOA measurement approach based on correlative spectrum analysis and processing implemented by using S2 materials was reported in [122]. The received microwave signal is applied to drive two EOMs placed in the two arms of a Mach–Zehnder interferometer, with the microwave power spectrum and the TDOA being recorded to the generated optical sidebands. Since the power level of the optical sidebands is linked to the TDOA, a ratio between the sum power and the difference power of the generated optical sidebands can be used to calculate the AOA of a microwave signal.

6.2. Near-field AOA measurement

In the near-field scenarios, the distance between the source and the measurement system is short and each antenna element in the measurement array receives the microwave signal at a different angle. The AOA or location is determined jointly by a set of hyperbolic curves with each defined via the TDOA between every two photonic receiving units.

Several photonic approaches to AOA measurement or location detection have been demonstrated [123–125]. A fiber-connected ultrawideband (UWB) sensing network for high-resolution localization, for example, was demonstrated based on optical time-division multiplexing (OTDM) [124]. A central station and several units were installed and connected via single-mode fibers, where a proper time delay was specified between every two units to map the UWB pulses received by different sensor nodes into different time slots. By using mapping approaches or geometric techniques, the target location was estimated with a spatial resolution as high as 3.9 cm for two-dimensional (2D) localization in an experiment. An improved fiber-connected network for localizing both pulsed and non-pulsed microwave signal sources was designed based on WDM [125]. The TDOAs were detected at a few sensing nodes allocated with different optical carriers and then utilized to define a set of hyperbolic curves for identifying the location of the source. A spatial resolution less than 17 cm was experimentally achieved for localizing a WiFi signal source.

Numerous electronic solutions have been proposed for AOA estimation or direction finding, capable of reaching a resolution of ±1° based on phase comparison [5]. In these electronic solutions, a uniform/nonuniform linear array, a circular array, or a rectangular array can be used. Meanwhile, advanced signal processing algorithms, such as the root-multiple signal classification (Root-MUSIC) algorithm and the maximum-likelihood algorithm, can also be employed for accuracy enhancement [126–128]. For instance, a direction-finding system using an 8-element circular array was demonstrated with an RMS accuracy of 1.2° [128]. In addition, an electronic commercial direction finder (Rohde&Schwarz DDF550) is capable of offering an RMS accuracy better than 1°, while covering a frequency range from 300 kHz to 6 GHz. The advantages of using photonic approaches are the large bandwidth and the

fiber-based remote architecture, which cannot be achieved using the state-of-the-art electronics.

7. Photonic measurements of other signal parameters

7.1. Time–frequency analysis

Recently, a few photonic approaches have also been developed to perform time–frequency analysis based on Fourier transform, short-time Fourier transform (STFT), wavelet transform, or Fourier cosine transform [129–131]. In principle, the time–frequency analysis of a microwave signal can be done by first slicing the signal and shaping it using an optical filter and then converting it to the frequency domain using a dispersive element such as a dispersive fiber or a chirped FBG.

In [129], a photonic STFT was realized using a temporal pulse-shaping system consisting of an array of linearly chirped FBGs, with each FBG serving as a dispersive element for a particular time window to perform a real-time Fourier transform. In [130], a 2D array of linearly chirped FBGs was employed to implement wavelet transform, such as the Mexican hat wavelet. A photonic Fourier cosine transform was also successfully performed with the assistance of a two-tap photonic microwave filter [131].

7.2. Compressive sensing for a spectrally sparse signal

The compressive sensing (CS) is a technique developed to reduce the sampling rate for the measurement of a spectrally sparse signal [132]. In recent years, a number of photonic-assisted CS approaches have been proposed [133–143]. In a photonic-assisted CS system, the random modulation, demodulation, or measurement is realized by applying a pseudorandom binary sequence (PRBS) to interact with the microwave signal in the optical domain.

As an example, in [139] a wideband analog-to-digital convertor (ADC) based on photonic CS was reported with a sampling rate far below the Nyquist rate of the original signal. In the system, a microwave signal with a sparse spectrum is slowed down in the time domain by using a photonic time stretcher. The signal is then downsampled and reconstructed by a photonic CS module based on random demodulation. In [142], a photonic system was utilized for acquiring a radar signal. A random measurement matrix is first generated to compress the spectrum of the radar signal. Then, the radar signal modulated on the optical carrier is optically mixed with a PRBS signal by incorporating an IQ modulator and a PD with a bandwidth of 10 GHz. The output signal from the PD is processed by a low-pass filter and then by an offline digital signal processor to recover the radar signal. With the assistance of the sliding window-based algorithm, a rectangular pulse, a linear frequency-modulated pulse, and a pulse stream were acquired and reconstructed faithfully in an experiment.

7.3. Phase-noise measurement

High-performance phase-noise measurement [144–148] is indispensable for designing and fabricating low phase-noise microwave sources that are essential in virtually all electronic systems. By introducing a long time delay in the optical domain and performing optical mixing between the original and the delayed signals, the phase information can be extracted. A photonic measurement system based on this technique is capable of providing a wideband measurement with a high sensitivity.

In [147], a photonic approach to phase-noise measurement using a multifunctional microwave photonic processor was demonstrated. Thanks to the use of the microwave photonic processor, the EO conversion, photonic time delay, and phase control of the output microwave signal can be simultaneously realized, relieving the requirement on an accurate phase control over a large bandwidth for phase-noise measurement. The operation was validated by an experiment in which the phase-noise measurement for a frequency range from 5 to 40 GHz was demonstrated with a low phase-noise floor, such as -130 dBc Hz^{-1} @ 10 kHz offset at 10 GHz [147]. More recently, a configuration based on photonic downconversion was proposed and experimentally demonstrated [148]. The phase-noise measurement for a frequency range from 5 to 40 GHz with a nearly constant phase-noise floor over the entire range was demonstrated. For example, the phase-noise floor was measured to be –123 dBc Hz^{-1} @1 kHz offset or –137 dBc Hz^{-1} @ 10 kHz offset at 10 GHz [148].

For phase-noise measurement, commercial instruments based on electronics are readily available, such as Keysight E5052B and Rohde&Schwarz FSWP50. Taking the latter as an example, it combines a low-noise internal source and the cross correlation technology to ensure a high sensitivity for phase-noise measurement within a frequency range from 10 MHz to 50 GHz. A phase-noise level of –147 dBc Hz^{-1} or –127 dBc Hz^{-1} @ 10 kHz offset can be provided at 10 GHz, when using cross correlation or not, which will inevitably increase as the microwave frequency grows. Hence, the photonic measurement approaches [147, 148] are able to provide a competitive performance in terms of phase-noise floor, with a nearly constant value over a frequency range of 35 GHz, from 5 to 40 GHz.

8. Functional measurement system: photonic microwave radars

In addition to the photonic measurements to microwave signal parameters, functional measurement systems enabled by photonics have been considerably developed within recent years, such as fully photonics-based coherent radars for remote ranging, positioning and imaging [24, 26, 149–153].
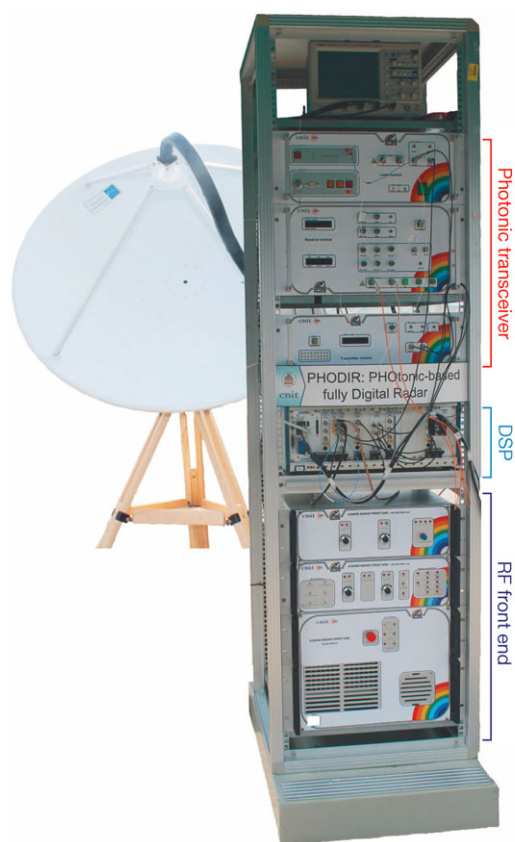
Figure 16 Fully photonics-based coherent radar. (DSP: digital signal processing; RF: radio frequency) (reprinted from [24] with copyright permission).

8.1. A fully photonics-based radar

For conventional electronics-based radars, most digital and microwave components used today face inherent electronic speed limitations and large noises at high frequencies, particularly the frequency synthesizers and the ADCs. In contrast, photonics enables microwave processing and measurements with high speed or large bandwidth.

To transfer these distinct advantages of photonics into a functional measurement system, a fully photonics-based coherent radar was firstly demonstrated in [24], where a photonic transceiver using a shared MLL was designed for generating the transmitting microwave signal and for sampling the echo signal. As illustrated in Fig. 16, the photonic radar consists of a laser module, a transmitter module, a receiver module, a digital processing module, and an RF frontend. The laser module provides a shared MLL with intrinsic high stability in phase and amplitude. In the photonic transmitter module, two comb lines from the MLL are selected, one being modulated by a baseband radar signal and the other being frequency shifted. After optical heterodyning, a microwave signal with a high-quality microwave carrier up to tens of gigahertz and an arbitrary temporal waveform carried by the microwave carrier is generated. At the photonic receiver, the high-frequency echo signal is sampled and directly digitized with very low time jitters. Assisted by multiple low-speed electrical ADCs and a post digital signal-processing stage, high performance was achieved for a photonic microwave radar in the field trial.

According to the results obtained from the field trial, the photonic radar outperforms the state-of-the-art electronic radars at a carrier frequency above 2 GHz. Key specifications of the photonic radar were shown in Table 1 of [24], including a tunable carrier frequency up to 40 GHz, a signal/sampling jitter less than 10 fs, and a 7-bit effective number for the carrier frequency up to 40 GHz. When operating at 9.9 GHz, the photonic radar provided a range resolution of 150 m for a target distance of ∼5.5 km and a resolution of 2 km h^{-1} for a target radial velocity of ∼96 km h^{-1}.

8.2. Photonic radars with versatile functionalities

Furthermore, radar systems with versatile functionalities are expected for diverse applications. The architecture proposed in [24] can be upgraded to provide versatile functionalities, such as multiband and multiwaveform systems for providing multispectral imaging, long-range target detection and tracking. In [149], a dual-band transceiver operating in the X- and S-bands was designed and validated for the detection of moving targets. Another field trial was carried out to detect both cooperating and noncooperating targets in the maritime scenario in [150]. From those results, it is further expected that a multispectral observation and a resolution improvement can be realized by gathering information from different bands or by data fusion.

An innovative coherent radar-lidar architecture has also been proposed to provide versatile functionalities. For example, an architecture for integrating a photonic radar (e.g., X-band and Ku-band) and a lidar with a tunable tone separation was designed [151] and [152], characterized by the manifold advantages from both radar and lidar. Experimentally, different tone separations or spacings of 10, 40, 80, or 160 GHz were specified for velocity measurement. A photonic radar operating at much higher frequency (e.g., 250 GHz [153]) was also proposed, which is very attractive for niche sensing applications.

9. Discussions

9.1. Advantages

According to the discussions given in Sections 1–7, photonic microwave measurement techniques do have notable advantages including large instantaneous bandwidth, wide frequency coverage, low frequency-dependent loss and immunity to EMI, thanks to the intrinsic features offered by photonics. When it comes to the system design, other distinct features including remote distribution via optical fiber and parallel processing based on WDM are also impressive.

Here, we would like to clarify in more detail concerning the large instantaneous bandwidth and wide frequency coverage. As for the real-time or instantaneous frequency measurement, photonic approaches based on optical comb filters are capable of achieving a large instantaneous bandwidth greater than 20 GHz [38–45]. As can be seen from Table 1, however, the analysis bandwidth of today's real-time microwave signal analyzers is likely to be limited to ~500 MHz. As for frequency coverage, photonic measurement solutions can scan over a frequency range greater than 1 THz in principle, without any limit on the frequency tuning or frequency multiplication of a LO signal used for heterodyning detection in electrical solutions. In a state-of-the-art microwave spectrum analyzer such as Rohde&Schwarz FSW85, the upper limit of the frequency range is 85 GHz. Also, the photonic DFS measurement approaches [112–114] are totally independent of the frequency of the microwave carrier, providing a frequency coverage or a frequency tuning range greater than 100 GHz in theory and an experimentally validated measurement range from 10 to 38 GHz. Table 2 summaries the performance specifications of a few selected photonic microwave measurement systems.

9.2. Disadvantages

Like current challenges against widespread applications of microwave photonics reviewed in [154], there are still critical disadvantages to photonic microwave measurements of practical interest, which are mainly associated with the resolution, stability and sensitivity.

First, the frequency of an optical carrier (e.g., 190 THz) is several orders of magnitude higher than that of a microwave carrier (e.g., 20 GHz), indicating that basically the resolution in the optical domain is approximate 10 000 times poorer than that in the microwave domain. It is evident that the resolution is limited to be 0.01 nm (i.e., 1.25 GHz [28]) when an OSA is used for spectrum analysis, despite a frequency measurement range of 2.5 THz or wider. In most photonic measurement solutions, therefore, the resolution has been improved at the cost of a reduction in the frequency coverage. As shown in Table 2, a resolution from hundreds of megahertz to several megahertz is regarded as an excellent value in the optical domain, but an unfavorable one in the electrical domain.

The resolution or accuracy can be further improved in photonic approaches for IFM, however, it is still at the level of tens or hundreds of megahertz within a wide and unambiguous frequency measurement range, according to the experimental results obtained from a large number of photonic approaches. However, in electronic solutions, the achievable resolution is 1 MHz for IFM receivers, tens of kilohertz or less for real-time microwave signal analyzers, or 0.1 Hz for microwave spectrum analyzers operating in the scanning mode. Such disadvantages or limitations outlined in several selected papers are also shown in Table 2 for a clear comparison.

Table 2 Specifications of selected photonic systems to microwave measurements

Reference	Functionality	Instantaneous bandwidth or measurement coverage[a]	Resolution or accuracy[a]
[29], 1999	Scanning spectrum analysis	Up to 40 GHz	90 MHz
[37], 2016	Scanning spectrum analysis	9~38 GHz	±1 MHz
[39], 2009	Instantaneous frequency measurement	1~26 GHz	±200 MHz
[45], 2013	Instantaneous frequency measurement	5~20 GHz	±100 MHz and ±80 MHz for a pulsed and a CW signal
[58], 2014	Instantaneous frequency measurement	0.04~40 GHz	±100 MHz
[59], 2015	Instantaneous frequency measurement	0~40 GHz	318.9 MHz
[116], 2012	Angle-of-arrival detection	−160° to 40°	±2.5° @ 18 GHz
[117], 2014	Angle-of-arrival detection	5° to 165°	±3.1° @ 12.5 GHz
[112,113], 2015	Doppler frequency shift measurement	Up to 30 GHz	±60 Hz
[95], 2012	Microwave channelization	3.75 ~ 7.25 GHz	125 kHz
[100], 2013	Microwave channelization	0~20 GHz	2 MHz
[24], 2014	Photonic radar	Up to 40 GHz	@ 9.9 GHz: a distance error of 100m and a radial velocity error of 1 km h^{-1}
[149], 2015	Photonic radar	S-band and X-band	Precision of velocity measurement: 0.3 m s^{-1} in S-band and 0.08 m s^{-1} in X-band

[a]within one unambiguous/monotonic range

Secondly, the operation stability is usually sensitive to the wavelength drift of lasers and the susceptibility of photonic devices in ambient environments. If no stabilization control is used, for example, there will be some wavelength drifts from hundreds of hertz to hundreds of megahertz in commercial laser sources. Such drifts even less than 10 MHz would bring crucial performance degradation to microwave processing and measurements both in amplitude and in phase, despite little degradation on conventional WDM communications.

Thirdly, the relatively weak sensitivity might also be regarded as an obstacle against practical applications. Basically, EO modulation and OE conversion are needed during the procedure of photonic microwave measurements, which would severely degrade the sensitivity because of low modulation/conversion efficiency and high nonlinear noises.

Those disadvantages above primarily arise from the premature technology level of photonic microwave measurements. On the one hand, currently, limited elements, unsophisticated architectures and simple post signal processing are employed for implementing photonic microwave measurements. On the other hand, as a mature technology, electronic solutions use complicated cascaded/parallel systems and powerful digital post signal processing and thus provide high resolution and impressive sensitivity. Three examples are selected to clarify this point as follows. First, for the electronic IFM, a host of phase discriminators based on many delay lines work together for offering both larger frequency coverage and finer resolution [5,6,79–82], rather than only one or two phase discriminators in photonic approaches. Secondly, two stages or more are designed for electronic channelizers, such as an RF, an IF, and a digital channelization stages [106, 107], capable of offering fine resolution over a relatively large frequency range. Moreover, advanced algorithms and digitalized means have been widely utilized for the electronic microwave measurements, which further enhance the resolution, sensitivity, and stability.

10. Future prospects

Both notable advantages and critical disadvantages of photonic microwave measurements have been discussed in Section 9. For future prospects, first, the challenges regarding the resolution, stability and sensitivity, should be addressed by great efforts to pave the way for widespread applications. More importantly, there are other impactful technical prospects for performing photonic microwave measurements, such as the PICs and software-defined solutions.

10.1. Photonic integrated circuits for microwave measurements

To date, most of the photonic microwave approaches and systems are implemented using discrete optoelectronic components and devices connected by waveguides or fiber pigtails, which might be considered as bulky, susceptible, and power consuming, while lacking flexibility in some scenarios. Fortunately, like electronic integrated circuits, PICs have been developed to provide promising solutions to overcome these limitations. By consolidating many elements or units on a chip or in a package, PICs considerably facilitate operational stability, compact footprint, and low power consumption.

Recently, both for general-purpose microwave photonics systems and photonic microwave measurement systems, some onchip devices and systems based on PICs have been demonstrated, which can be categorized into several major materials or technologies including InP, GaAs, polymer, $LiNbO_3$, silica, silicon-on-insulator (SOI), Si_3N_4/SiO_2, and As_2S_3 [15,19,28,37,46–50,59,77,155–163]. Multiple laser sources, modulators, amplifiers, couplers, resonators, gratings, and PDs can be integrated on a monolithic chip of the size of a square millimeter or less. As an example, a photonic microwave channelizer comprised of active integrated filters was fabricated on a single chip on InP wafer with a size of ∼9 mm for coupler separation [163], with the assistance of microelectronic processing techniques. Integrated lenses, resonators, and nonlinear waveguides have also been employed to perform spectrum analysis and IFM [31,37,46–50,59,77]. Table 3 shows a few microwave measurement systems based PICs to present the functionalities, key components and materials used.

10.2. Software-defined solutions for photonic microwave measurements

With the rapid development of PICs, software-defined solutions are regarded as another emerging technology for performing microwave measurements, like the software-defined radio widely developed to implement multiservice, multistandard, multiband or programmable systems based on shared and simplified hardware [164]. Therefore, the system complexity and the SWaP-C (size, weight, power, and cost) will be dramatically reduced.

For this reason, software-defined solutions are really desirable for microwave photonics and photonic microwave measurements. In [165], a programmable photonic microwave filter fabricated on a monolithic chip was reported. Software-defined photonic transceivers and radars have also been developed to support multiple frequency bands and to provide multiple resolutions or multiple functionalities [149, 166–170], which indicate an innovative breakthrough for new-generation radar. Software-defined satellite payloads based on microwave photonics are becoming attractive and highly feasible for future [171]. Very recently, for general-purpose applications, software-defined processor architecture [172] and programmable processor chips [173, 174] are reported for signal processing and measurements. In brief, software-defined solutions are expected to greatly facilitate photonic microwave measurements and microwave photonics with low complexity and flexible reconfigurability in diverse applications.

Table 3 Selected microwave measurement systems based on PICs

Reference	Functionality	Key component	Material
[31], 2009	Scanning spectrum analysis	Integrated echelle diffractive grating	InGaAsP–InP
[37], 2016	Scanning spectrum analysis	Nonlinear rib waveguide	As_2S_3
[46], 2010; [47], 2013	Instantaneous frequency measurement	Optical ring resonator	Si_3N_4/SiO_2
[48], 2011; [49], 2013	Instantaneous frequency measurement	Ring-assisted Mach–Zehnder interferometer	InP
[59], 2015	Instantaneous frequency measurement	Silicon strip waveguide	Silicon
[77], 2015	Instantaneous frequency measurement	Microdisk resonator	Silicon
[84], 2006	Microwave channelization	Integrated Fabry–Pérot and Fresnel lens	Silica on silicon
[161], 2010; [119], 2012	Angle-of-arrival detection	Optical ring resonator and Mach–Zehnder interferometer	Si_3N_4/SiO_2

11. Conclusions

In this article, we have provided a comprehensive overview of recent advances in photonic microwave measurements, including microwave spectrum analysis, instantaneous frequency measurement, microwave channelization, DFS measurement, AOA detection, phase-noise measurement, and microwave sensing and ranging (e.g., radar). The performance of photonic solutions was then discussed with both advantages and disadvantages, compared with that of conventional electronic measurement solutions.

Photonic microwave measurement techniques provide superior performance in terms of instantaneous bandwidth, frequency coverage, and frequency-dependent loss. However, the resolution, stability, and sensitivity are relatively poorer, which is mainly caused by the use of discrete photonic components, simple post signal processing units or algorithms, and relatively unsophisticated architectures.

An enabling solution to enhance the resolution, stability, and sensitivity is to implement the photonic microwave measurement systems using PICs. The fast advancement in PICs, especially the recent development in silicon photonics, would allow photonic microwave measurement systems to operate with not only a broad bandwidth and low loss, but also favorable resolution, high sensitivity and excellent stability. Then, the software-defined architecture based on PICs would further facilitate photonic measurement functionalities with low complexity and flexible reconfigurability. These trends will make photonic microwave measurement techniques a practical solution for widespread applications in the foreseeable future.

Xihua Zou is a Professor with the Center for Information Photonics and Communications, Southwest Jiaotong University, China. He received the Ph.D. degree from Southwest Jiaotong University, China, in 2009. Since October 2014, he has been working as a Humboldt Research Fellow in the Institute of Optoelectronics, University of Duisburg-Essen, Germany. He was a visiting researcher and a joint training Ph.D. student in the Microwave Photonics Research Laboratory, University of Ottawa, Canada, in 2011 and 2007–2008. His research interests include microwave photonics, radio over fiber, and optical communications.

**Bing Lu** received the B.S. degree from the Zhoukou Normal University, China, in 2010. He is currently working toward the Ph.D. degree in the School of Information Science and Technology, Southwest Jiaotong University, China. His research interests include microwave photonics and optical communications.
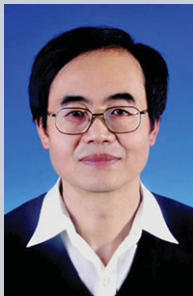
Wei Pan is a Professor and the Dean of the School of Information Science and Technology, Southwest Jiaotong University, China. He received the Ph.D. degree from Southwest Jiaotong University, China. His research interests include semiconductor lasers, nonlinear dynamic systems, and optical communications.
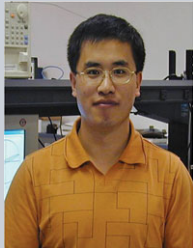
Lianshan Yan is a Professor and the Director of the Center for Information Photonics and Communications, Southwest Jiaotong University, China. He received the Ph.D. degree from the University of Southern California, United States. His research interests include optical communications and networks, microwave photonics, and optical sensors.

Andreas Stöhr is a Professor with the Institute of Optoelectronics, University of Duisburg-Essen, Germany. He received the Dipl. Ing. and the Dr. Ing. degrees in electrical engineering from Gerhard-Mercator Universität Duisburg (GMUD), Duisburg, Germany, in 1991 and 1997, respectively. In 1998 and 1999, he joined the Communications Research Laboratory, Ministry of Posts and Telecommunications, Japan. His research interests include III–V-based microwave photonic devices and applications, and microwave/millimeter-wave fiber-optic transmission systems.

Jianping Yao is a Distinguished University Professor and University Research Chair in the School of Electrical Engineering and Computer Science, University of Ottawa, Canada. With over 510 refereed publications, he has made seminal contributions to Microwave Photonics, including photonic-assisted microwave signal generation and microwave arbitrary waveform generation, microwave signal processing, photonic integrated circuits for ultrafast signal processing, and fiber-wireless communications. Prof. Yao is a Fellow of the IEEE, the Optical Society of America, and the Canadian Academy of Engineering.

References

[1] D. M. Pozar, Microwave Engineering, 3rd edition, (Wiley, 2004).

[2] J. Tsui, Microwave Receivers with Electronic Warfare Applications, (SciTech Publishing, 2005).

[3] G. H. Bryant, Principles of Microwave Measurements, revised edition, (IET, London, UK, 1993).

[4] M. Skolnik, Introduction to Radar Systems, (McGrawHill, NewYork, 2001).

[5] J. Tsui, Digital Techniques for Wideband Receivers, (SciTech Publishing, 2004).

[6] J. Tsui, Special Design Topics in Digital Wideband Receivers, (Artech House, 2014).

[7] M. Jankiraman, Design of Multi-Frequency CW Radars, (SciTech Publishing, 2007).

[8] R. J. Collier and A. D. Skinner, Microwave Measurements, 3rd edition, (IET, London, UK, 2007).

[9] V. Teppati, A. Ferrero and M. Sayed, Modern RF and Microwave Measurement Techniques, (Cambridge University Press, Cambridge, UK, 2013).

[10] A. Basu, An Introduction to Microwave Measurements, (CRC Press, Boca Raton, United States, 2015).

[11] A. J. Seeds and K. J. Williams, Microwave photonics, J. Lightwave Technol. **24**(12), 4628–4641 (2006).

[12] S. Tonda-Goldstein, D. Dolfi, A. Monsterleet, S. Formont, J. Chazelas, and J. P. Huignard, Optical signal processing in radar systems, IEEE Trans. Microw. Theory Techn. **54**(2),847–853 (2006).

[13] J. Capmany and D. Novak, Microwave photonics combines two worlds, Nature Photon. **1**(6), 319–330 (2007).

[14] M. E. Manka, Microwave photonics for electronic warfare applications, IEEE International Topical Meeting on Microwave Photonics, 275–278, 2008.

[15] L. A. Coldren, Photonic integrated circuits for microwave photonics, IEEE International Topical Meeting on Microwave Photonics, 1–4, 2010.

[16] G. Xiao and W. J. Bock, Photonic Sensing: Principles and Applications for Safety and Security Monitoring, (Wiley, 2012).

[17] V. Supradeepa, C. M. Long, R. Wu, F. Ferdous, E. Hamidi, D. E. Leaird, and A. M. Weiner, Comb-based radiofre-

quency photonic filters with rapid tunability and high selectivity, Nature Photon. **6**(3), 186–194 (2012).

[18] G. J. Schneider, J. A. Murakowski, C. A. Schuetz, S. Shi, and D. W. Prather, Radiofrequency signal-generation system with over seven octaves of continuous tuning, Nature Photon.**7**(2), 118–122 (2013).

[19] D. Marpaung, C. Roeloffzen, R. Heideman, A. Leinse, S. Sales, and J. Capmany, Integrated microwave photonics, Laser Photon. Rev. **7**(4), 506–538 (2013).

[20] R. W. Ridgway, J. Conway, and C. L. Dohrman, Microwave photonics: recent programs at DARPA, IEEE International Topical Meeting on Microwave Photonics, 286–289, (2013).

[21] J. Capmany, J. Mora, I. Gasulla, J. Sancho, J. Lloret, and S. Sales, Microwave photonic signal processing, J. Lightwave Technol. **31**(4),571–586 (2013).

[22] A. M. Fard, S. Gupta, and B. Jalali, Photonic time-stretch digitizer and its extension to real-time spectroscopy and imaging, Laser Photon. Rev. **7**(2), 207–263 (2013).

[23] V. Torres-Company and A. M. Weiner, Optical frequency comb technology for ultra-broadband radio-frequency photonics, Laser Photon. Rev. **8**(3), 368–393 (2014).

[24] P. Ghelfi, F. Laghezza, F. Scotti, G. Serafino, A. Capria, S. Pinna, D. Onori, C. Porzi, M. Scaffardi, A. Malacarne, V. Vercesi, E. Lazzeri, F. Berizzi, and A. Bogoni, A fully photonics-based coherent radar system, Nature **507**(7492), 341–345 (2014).

[25] V. J. Urick, K. J. Williams, and J. D. McKinney, Fundamentals of Microwave Photonics, (Wiley, 2015).

[26] X. Zou, X. Liu, W. Li, P. Li, W. Pan, L. Yan, and L. Shao, Optoelectronic oscillators (OEOs) to sensing, measurement, and detection, IEEE J. Quantum Electron. **52**(1), 0601116, (2016).

[27] R. Minasian, Ultra-wideband and adaptive photonic signal processing of microwave signals, IEEE J. Quantum Electron. **52**(1), 0600813, (2016).

[28] M. Pelusi, F. Luan, T. D. Vo, M. R. Lamont, S. J. Madden, D. A. Bulla, D. Y. Choi, B. Luther-Davies, and B. J. Eggleton, Photonic-chip-based radio-frequency spectrum analyzer with terahertz bandwidth, Nature Photon. **3**(3), 139–143 (2009).

[29] S. Winnall and A. Lindsay, A Fabry-Perot scanning receiver for microwave signal processing, IEEE Trans. Microw. Theory Techn. **47**(7), 1385–1390 (1999).

[30] P. Rugeland, Z. Yu, C. Sterner, O. Tarasenko, G. Tengstrand, and W. Margulis, Photonic scanning receiver using an electrically tuned fiber Bragg grating, Opt. Lett. **34**(24), 3794–3796 (2009).

[31] H. Guo, G. Xiao, N. Mrad, and J. Yao, Measurement of microwave frequency using a monolithically integrated scannable echelle diffractive grating, IEEE Photon. Technol. Lett. **21**(1), 45–47 (2009).

[32] B. Vidal, T. Mengual, and J. Marti, Photonic technique for the measurement of frequency and power of multiple microwave signals, IEEE Trans. Microw. Theory Techn. **58**(11), 3103–3108 (2010).

[33] S. Zheng, S. Ge, X. Zhang, H. Chi, and X. Jin, High-resolution multiple microwave frequency measurement based on stimulated Brillouin scattering, IEEE Photon. Technol. Lett. **24**(13), 1115–1117 (2012).

[34] S. Preußler, A. Wiatrek, K. Jamshidi, and T. Schneider, Brillouin scattering gain bandwidth reduction down to 3.4 MHz, Opt. Express **19**(9), 8565–8570 (2011).

[35] S. Preussler and T. Schneider, Attometer resolution spectral analysis based on polarization pulling assisted Brillouin scattering merged with heterodyne detection, Opt. Express **23**(20), 26879–26887 (2015).

[36] S. Preussler and T. Schneider, Stimulated Brillouin scattering gain bandwidth reduction and applications in microwave photonics and optical signal processing, Opt. Eng. **55**(3), 031110 (2016).

[37] H. Jiang, D. Marpaung, M. Pagani, K. Vu, D. Y. Choi, S. J. Madden, L. Yan, and B. J. Eggleton, Wide-range, high-precision multiple microwave frequency measurement using a chip-based photonic Brillouin filter, Optica **3**(1), 30–34 (2016).

[38] H. Chi, X. Zou, and J. Yao, An approach to the measurement of microwave frequency based on optical power monitoring, IEEE Photon. Technol. Lett. **20**(14), 1249–1251 (2008).

[39] X. Zou, H. Chi, and J. Yao, Microwave frequency measurement based on optical power monitoring using a complementary optical filter pair, IEEE Trans. Microw. Theory Techn. **57**(2), 505–511 (2009).

[40] M. Drummond, P. Monteiro, and R. Nogueira, Photonic RF instantaneous frequency measurement system by means of a polarization domain interferometer, Opt. Express **17**(7), 5433–5438 (2009).

[41] S. Pan and J. Yao, Instantaneous microwave frequency measurement using a photonic microwave filter pair, IEEE Photon. Technol. Lett. **22**(19), 1437–1439 (2010).

[42] X. Zou, W. Pan, B. Luo, and L. Yan, Photonic instantaneous frequency measurement using a single laser source and two quadrature optical filters, IEEE Photon. Technol. Lett. **23**(1), 39–41 (2011).

[43] X. Zou, W. Pan, B. Luo, and L. Yan, Full-scale phase demodulation approach for photonic instantaneous frequency measurement, Opt. Lett. **35**(16), 2747–2749 (2010).

[44] S. Pan, J. Fu, and J. Yao, Photonic approach to the simultaneous measurement of the frequency, amplitude, pulse width, and time of arrival of a microwave signal, Opt. Lett. **37**(1), 7–9 (2012).

[45] B. Lu, W. Pan, X. Zou, B. Luo, L. Yan, X. Liu, and S. Xiang, Photonic frequency measurement and signal separation for pulsed/CW microwave signals, IEEE Photon. Technol. Lett. **25**(5), 500–503 (2013).

[46] D. Marpaung, C. Roeloffzen, A. Leinse, and M. Hoekman, A photonic chip based frequency discriminator for a high performance microwave photonic link, Opt. Express **18**(26), 27359–27370 (2010).

[47] D. Marpaung, On-chip photonic-assisted instantaneous microwave frequency measurement system, IEEE Photon. Technol. Lett. **25**(9), 837–840 (2013).

[48] J. S. Fandino, J. D. Domenech, P. Munoz, and J. Capmany, Integrated InP frequency discriminator for phase-modulated microwave photonic links, Opt. Express **21**(3), 3726–3736 (2013).

[49] J. S. Fandino and P. Munoz, Photonics-based microwave frequency measurement using a double-sideband suppressed-carrier modulation and an InP integrated

ring-assisted Mach–Zehnder interferometer filter, Opt. Lett. **38**(21), 4316–4319 (2013).

[50] J. S. Fandino and P. Munoz, Analysis of system imperfections in a photonics-assisted instantaneous frequency measurement receiver based on a dual-sideband suppressed-carrier modulation, J. Lightwave Technol. **33**(2), 293–303 (2015).

[51] Z. Li, B. Yang, H. Chi, X. Zhang, S. Zheng, and X. Jin, Photonic instantaneous measurement of microwave frequency using fiber Bragg grating, Opt. Commun. **283**(3), 396–399 (2010).

[52] Z. Li, C. Wang, M. Li, H. Chi, X. Zhang, and J. Yao, Instantaneous microwave frequency measurement using a special fiber Bragg grating, IEEE Microw. Wirel. Compon. Lett. **21**(1), 52–54 (2011).

[53] N. Sarkhosh, H. Emami, L. Bui, and A. Mitchell, Reduced cost photonic instantaneous frequency measurement system, IEEE Photon. Technol. Lett. **20**(18), 1521–1523 (2008).

[54] H. Emami, N. Sarkhosh, L. Bui, and A. Mitchell, Amplitude independent RF instantaneous frequency measurement system using photonic Hilbert transform, Opt. Express **16**(18), 13707–13712 (2008).

[55] L. Bui, M. Pelusi, T. D. Vo, N. Sarkhosh, H. Emami, B. J. Eggleton, and A. Mitchell, Instantaneous frequency measurement system using optical mixing in highly nonlinear fiber, Opt. Express **17**(25), 22983–22991 (2009).

[56] L. Bui, N. Sarkhosh, and A. Mitchell, Photonic instantaneous frequency measurement: parallel simultaneous implementations in a single highly nonlinear fiber, IEEE Photon. J. **3**(5), 915–925 (2011).

[57] L. Bui and A. Mitchell, Amplitude independent instantaneous frequency measurement using all optical technique, Opt. Express **21**(24), 29601–29611 (2013).

[58] H. Emami and M. Ashourian, Improved dynamic range microwave photonic instantaneous frequency measurement based on four-wave mixing, IEEE Trans. Microw. Theory Techn. **62**(10), 2462–2470 (2014).

[59] M. Pagani, B. Morrison, Y. Zhang, A. Casas-Bedoya, T. Aalto, M. Harjanne, M. Kapulainen, B. J. Eggleton, and D. Marpaung, Low-error and broadband microwave frequency measurement in a silicon chip, Optica **2**(8), 751–756 (2015).

[60] L. V. Nguyen and D. B. Hunter, A photonic technique for microwave frequency measurement, IEEE Photon. Technol. Lett. **18**(10), 1188–1190 (2006).

[61] X. Zou and J. Yao, An optical approach to microwave frequency measurement with adjustable measurement range and resolution, IEEE Photon. Technol. Lett. **20**(23), 1989–1991 (2008).

[62] X. Zou and J. Yao, Microwave frequency measurement with improved measurement range and resolution, Electron. Lett. **45**(10), 497–498 (2009).

[63] X. Zhang, H. Chi, X. Zhang, S. Zheng, X. Jin, and J. Yao, Instantaneous microwave frequency measurement using an optical phase modulator, IEEE Microw. Wirel. Compon. Lett. **19**(6), 422–424 (2009).

[64] J. Li, S. Fu, K. Xu, J. Zhou, P. Shum, J. Wu, and J. Lin, Photonic-assisted microwave frequency measurement with

higher resolution and tunable range, Opt. Lett. **34**(6), 743–745 (2009).

[65] M. Attygalle and D.B. Hunter, Improved photonic technique for broadband radio-frequency measurement, IEEE Photon. Technol. Lett. **21**(4), 206–208 (2009).

[66] J. Zhou, S. Fu, S. Aditya, P. P. Shum, and C. Lin, Instantaneous microwave frequency measurement using photonic technique, IEEE Photon. Technol. Lett. **21**(15), 1069–1071 (2009).

[67] J. Zhou, S. Fu, P. P. Shum, S. Aditya, L. Xia, J. Li, X. Sun and K. Xu, Photonic measurement of microwave frequency based on phase modulation, Opt. Express **17**(9), 7217–7221 (2009).

[68] X. Zou, S. Pan, and J. Yao, Instantaneous microwave frequency measurement with improved measurement range and resolution based on simultaneous phase modulation and intensity modulation, J. Lightwave Technol. **27**(23), 5314–5320 (2009).

[69] S. Fu, J. Zhou, P. P. Shum, and K. Lee, Instantaneous microwave frequency measurement using programmable differential group delay (DGD) modules, IEEE Photon. J. **2**(6), 967–973 (2010).

[70] W. Li, N. H. Zhu, and L. X. Wang, Reconfigurable instantaneous frequency measurement system based on dual-parallel Mach–Zehnder modulator, IEEE Photon. J. **4**(2), 427–436 (2012).

[71] W. Li, N. H. Zhu, and L. X. Wang, Brillouin-assisted microwave frequency measurement with adjustable measurement range and resolution, Opt. Lett. **37**(2), 166–168 (2012).

[72] X. Zou, W. Pan, B. Luo, and L. Yan, Dispersion-induced-loss-independent photonic instantaneous frequency measurement using remote-fiber-based tunable microwave filter, IEEE Photon. Technol. Lett. **22**(15), 1090–1092 (2010).

[73] S. Pan and J. Yao, Instantaneous microwave frequency measurement using a photonic microwave filter pair, IEEE Photon. Technol. Lett. **22**(19), 1437–1439 (2010).

[74] J. Zhou, S. Aditya, P. P. Shum, and J. Yao, Instantaneous microwave frequency measurement using a photonic microwave filter with an infinite impulse response, IEEE Photon. Technol. Lett. **22**(10), 682–684 (2010).

[75] J. Niu, S. Fu, K. Xu, J. Zhou, S. Aditya, J. Wu, P. P. Shum, and J. Lin, Instantaneous microwave frequency measurement based on amplified fiber-optic recirculating delay loop and broadband incoherent light source, J. Lightwave Technol. **29**(1), 78–84 (2011).

[76] K. Xu, J. Dai, R. Duan, Y. Dai, Y. Li, J. Wu, and J. Lin, Instantaneous microwave frequency measurement based on phase-modulated links with interferometric detection, IEEE Photon. Technol. Lett. **23** (18), 1328–1330 (2011).

[77] L. Liu, F. Jiang, S. Yan, S. Min, M. He, D. Gao, and J. Dong, Photonic measurement of microwave frequency using a silicon microdisk resonator, Opt. Commun. **335**, 266–270 (2015).

[78] G. H. Smith, D. Novak, and Z. Ahmed, Overcoming chromatic-dispersion effects in fiber-wireless systems incorporating external modulators, IEEE Trans. Microw. Theory Techn. **45**(8), 1410–1415 (1997).

[79] P. W. East, Fifty years of instantaneous frequency measurement, IET Radar, Sonar Navig. **6**(2), 112–122 (2012).

[80] M. T. de Melo, B. G. M. de Oliveira, I. Llamas-Garro, and M. Espinosa-Espinosa, Radio frequency identification from system to applications, Ch. 14, (InTech, 2013).

[81] AN/WLR-1H(V)7 - Wide Band Systems: http://www.widebandsystems.com/Publications/Data%20Sheets/ANWLR1Hv7.pdf, accessed: April, 2016.

[82] DR058-F1, 2-18 GHz instantaneous frequency measurement unit: http://www.teledynedefence.co.uk/pdf/DR058-F1.pdf, accessed: April, 2016.

[83] W. Wang, R. L. Davis, T. J. Jung, R. Lodenkamper, L. J. Lembo, J. C. Brock, and M. C. Wu, Characterization of a coherent optical RF channelizer based on a diffraction grating, IEEE Trans. Microw. Theory Techn. **49**(10), 1996–2001 (2001).

[84] S. T. Winnall, A. Lindsay, M. W. Austin, J. Canning, and A. Mitchell, A microwave channelizer and spectroscope based on an integrated optical Bragg-grating Fabry-Perot and integrated hybrid Fresnel lens system, IEEE Trans. Microw.Theory Techn. **54**(2), 868–872 (2006).

[85] J. M. Heaton, C. D. Watson, S. B. Jones, M. M. Bourke, C. M. Boyne, G. W. Smith, and D. R. Wight, Sixteen channel (1 to 16 GHz) microwave spectrum analyzer device based on a phased-array of GaAs/AlGaAs electro-optic waveguide delay lines, Proc. SPIE **3278**, 245–251 (1998).

[86] D. Hunter, L. Edvell, and M. Englund, Wideband microwave photonic channelised receiver, IEEE International Topical Meeting on Microwave Photonics, 249–252, 2005.

[87] A. P. Goutzoulis, Integrated optical channelizer, US Patent 7421168 (Sep. 2, 2008).

[88] F. A. Volkening, Photonic channelized RF receiver employing dense wavelength-division multiplexing, US Patent 7245833 (Jul. 17, 2007).

[89] X. Zou, W. Pan, B. Luo, and L. Yan, Photonic approach for multiple-frequency-component measurement using spectrally sliced incoherent source, Opt. Lett. **35**(3), 438–440 (2010).

[90] C. S. Bres, S. Zlatanovic, A. O. Wiberg, J. R. Adleman, C. K. Huynh, E. Jacobs, J. M. Kvavle, and S. Radic, Parametric photonic channelized RF receiver, IEEE Photon. Technol. Lett. **23**(6), 344–346 (2011).

[91] A. O. J. Wiberg, D. J. Esman, L. Liu, J. R. Adleman, S. Zlatanovic, V. Ataie, E. Myslivers, B. P. P. Kuo, N. Alic, E. W. Jacobs, and S. Radic, Coherent filterless wideband microwave/millimeter-wave channelizer based on broadband parametric mixers, J. Lightwave Technol. **32**(20), 3609–3617 (2014).

[92] Z. Li, X. Zhang, H. Chi, S. Zheng, X. Jin, and J. Yao, A reconfigurable microwave photonic channelized receiver based on dense wavelength-division multiplexing using an optical comb, Opt. Commun. **285**, 2311–2315 (2012).

[93] L. X. Wang, N. H. Zhu, W. Li, H. Wang, J. Y. Zheng, and J. G. Liu, Polarization division multiplexed photonic radio-frequency channelizer using an optical comb, Opt. Commun. **286**, 282–287 (2013).

[94] X. Xie, Y. Dai, Y. Ji, K. Xu, Y. Li, J. Wu, and J. Lin, Broadband photonic radio-frequency channelization based on a 39-GHz optical frequency comb, IEEE Photon. Technol Lett. **24**(8), 661–663 (2012).

[95] X. Xie, Y. Dai, K. Xu, J. Niu, R. Wang, L. Yan, and J. Lin, Broadband photonic RF channelization based on coherent optical frequency combs and I/Q demodulators, IEEE Photon. J. **4**(4), 1196–1202 (2012).

[96] X. Zou, W. Li, W. Pan, L. Yan, and J. Yao, Photonic-assisted microwave channelizer with improved channel characteristics based on spectrum-controlled stimulated Brillouin scattering, IEEE Trans. Microw. Theory Techn. **61**(9), 3470–3478 (2013).

[97] W. Xu, D. Zhu, and S. Pan, Coherent photonic RF channelization based on stimulated Brillouin scattering, IEEE International Topical Meeting on Microwave Photonics, WeB-2, 2015.

[98] R. K. Mohan, T. Chang, M. Tian, S. Bekker, A. Olson, C. Ostrander, A. Khallaayoun, C. Dollinger, W. Babbitt, Z. Cole, R. R. Reibel, K. D. Merkel, Y. Sun, R. Cone, F. Schlottau, and K. H. Wagner, Ultra-wideband spectral analysis using S2 technology, J. Lumin. **127**(1), 116–128 (2007).

[99] C. Wang and J. Yao, Ultrahigh-resolution photonic-assisted microwave frequency identification based on temporal channelization, IEEE Trans. Microw. Theory Techn. **61**(12), 4275–4282 (2013).

[100] R. Li, H. Chen, Y. Yu, M. Chen, S. Yang, and S. Xie, Multiple-frequency measurement based on serial photonic channelization using optical wavelength scanning, Opt. Lett. **38**(22), 4781–4784 (2013).

[101] R. Li, H. Chen, C. Lei, Y. Yu, M. Chen, S. Yang, and S. Xie, Optical serial coherent analyzer of radio-frequency (OSCAR), Opt. Express **22**(11), 13579–13585 (2014).

[102] H. Chen, R. Li, C. Lei, Y. Yu, M. Chen, S. Yang, and S. Xie, Photonics-assisted serial channelized radio-frequency measurement system with Nyquist-bandwidth detection, IEEE Photon. J. **6**(6), 7903707 (2014).

[103] T. A. Nguyen, E. H. Chan, and R. A. Minasian, Photonic multiple frequency measurement using a frequency shifting recirculating delay line structure, J. Lightwave Technol. **32**(20), 3831–3838 (2014).

[104] W. G. Anderson, C. D. Webb, E. A. Spezio, and J. N. Lee, Advanced channelization for RF, microwave, and millimeter-wave applications, Proc. IEEE, **79**(3), 355–388 (1991).

[105] E. A. Spezio. Electronic warfare systems, IEEE Trans. Microw. Theory Techn. **50**(3), 633–644 (2002).

[106] D. Gupta, T. V. Filippov, A. F. Kirichenko, D. E. Kirichenko, I. V. Vrnik, A. Sahu, S. Sarwana, P. Shevchenko, A. Talalaevskii, and O. A. Mukhanov, Digital channelizing radio frequency receiver, IEEE Trans. Appl. Supercond. **17**(2), 430–437 (2007).

[107] J. P. Magalhaes, J. M. N. Vieira, R. Gomez-Garcia, and N. B. Carvalho, Bio-inspired hybrid filter bank for software-defined radio receivers, IEEE Trans. Microw. Theory Techn. **61**(4), 1455–1466 (2013).

[108] V. C. Chen, F. Li, S.-S. Ho, and H. Wechsler, Micro-Doppler effect in radar: phenomenon, model, and simulation study, IEEE Trans. Aerosp. Electron. Syst. **42**(1), 2–21 (2006).

[109] F. Alimenti, F. Placentino, A. Battistini, G. Tasselli, W. Bernardini, P. Mezzanotte, D. Radcio, V. Palazzari, S. Leone, A. Scaponi, N. Porzi, M. Comez, and L. Roselli, A low-cost 24GHz Doppler radar sensor for traffic monitoring

implemented in standard discrete-component technology, IEEE European Microwave Conference, 1441–1444, 2007.

[110] A. Tessmann, S. Kudszus, T. Feltgen, M. Riessle, C. Sklarczyk, and W. H. Haydl, Compact single-chip W-band FMCW radar modules for commercial high-resolution sensor applications, IEEE Trans. Microw. Theory Techn. **50**(12), 2995–3001 (2002).

[111] B. Mencia-Oliva, J. Grajal, O. A. Yeste-Ojeda, G. Rubio-Cidre, and A. Badolato, Low-cost CW-LFM radar sensor at 100 GHz, IEEE Trans. Microw. Theory Techn. **61**(2), 986–998 (2013).

[112] X. Zou, W. Li, B. Lu, W. Pan, L. Yan, and L. Shao, Photonic approach to wide-frequency-range high-resolution microwave/millimeter-wave Doppler frequency shift estimation, IEEE Trans. Microw. Theory Techn. **63**(4), 1421–1430 (2015).

[113] B. Lu, W. Pan, X. Zou, X. Yan, L. Yan, and B. Luo, Wideband Doppler frequency-shift measurement and direction ambiguity resolution using optical frequency shift and optical heterodyning, Opt. Lett. **40**(10), 2321–2324 (2015).

[114] B. Lu, W. Pan, X. Zou, Y. Pan, X. Liu, L. Yan, and B. Luo, Wideband microwave Doppler frequency shift measurement and direction discrimination using photonic I/Q detection, J. Lightwave Technol. **34**, DOI: 10.1109/JLT.2016.2580639 2016.

[115] B. Vidal, M. A. Piqueras, and J. Marti, Direction-of-arrival estimation of broadband microwave signals in phased-array antennas using photonic techniques, J. Lightwave Technol. **24**(7), 2741–2745 (2006).

[116] X. Zou, W. Li, W. Pan, B. Luo, L. Yan, and J. Yao, Photonic approach to the measurement of time-difference-of-arrival and angle-of-arrival of a microwave signal, Opt. Lett. **37**(4), 755–757 (2012).

[117] Z. Cao, Q. Wang, R. Lu, H. van den Boom, E. Tangdiongga, and A. Koonen, Phase modulation parallel optical delay detector for microwave angle-of-arrival measurement with accuracy monitored, Opt. Lett. **39**(6), 1497–1500 (2014).

[118] Z. Cao, H. P. van den Boom, R. Lu, Q. Wang, E. Tangdiongga, and A. Koonen, Angle-of-arrival measurement of a microwave signal using parallel optical delay detector, IEEE Photon. Technol. Lett. **19**(25), 1932–1935 (2013).

[119] M. Burla, C. G. Roeloffzen, L. Zhuang, D. Marpaung, M. R. Khan, P. Maat, K. Dijkstra, A. Leinse, M. Hoekman, and R. Heideman, System integration and radiation pattern measurements of a phased array antenna employing an integrated photonic beamformer for radio astronomy applications, Appl. Opt. **51**(7), 789–802 (2012).

[120] T. W. Tedesso, J. Calusdian, C. Sewing, and P. E. Pace, Wideband direction finding using a photonic robust symmetrical number system technique, Opt. Eng. **53**(11), paper.114109 (2014).

[121] R. Toole and M. P. Fok, Photonic implementation of a neuronal algorithm applicable towards angle-of-arrival detection and localization, Opt. Express **23**(12), 16133–16141 (2015).

[122] Z. Barber, C. Harrington, C. Thiel, W. R. Babbitt, and R. K. Mohan, Angle of arrival estimation using spectral interferometry, J. Lumin. **130**(9), 1614–1618 (2010).

[123] R. Llorente, M. Morant, N. Amiot, and B. Uguen, Novel photonic analog-to-digital converter architecture for precise localization of ultra-wide band radio transmitters, IEEE J. Sel. Area Comm. **29**(6), 1321–1327 (2011).

[124] J. Fu and S. Pan, Fiber-connected UWB sensor network for high-resolution localization using optical time-division multiplexing, Opt. Express **21**(18), 21218–21223 (2013).

[125] T. Yao, D. Zhu, S. Liu, F. Zhang, and S. Pan, Wavelength-division multiplexed fiber-connected sensor network for source localization, IEEE Photon. Technol. Lett. **26**(18), 1874–1877 (2014).

[126] B. A. Gershman, M. Rübsamen, and M. Pesavento, One- and two-dimensional direction-of-arrival estimation: an overview of search-free techniques, Signal Processing, **90**(5), 1338–1349 (2010).

[127] P. B. Kumar and G. R. Branner, Generalized analytical technique for the synthesis of unequally spaced arrays with linear, planar, cylindrical or spherical geometry, IEEE Trans. Antennas Propag. **53**(2), 621–634(2005).

[128] S. Murphy and M. P. Eyring, 2-18 GHz circular array interferometer DF antenna system, IEEE Antennas and Propagation Society International Symposium, **4**, 2332–2335, 1998.

[129] M. Li and J. Yao, All-optical short-time Fourier transform based on a temporal pulse-shaping system incorporating an array of cascaded linearly chirped fiber Bragg gratings, IEEE Photon. Technol. Lett. **23**(20), 1439–1441 (2011).

[130] M. Li and J. Yao, Ultrafast all-optical wavelet transform based on temporal pulse shaping incorporating a 2-D array of cascaded linearly chirped fiber Bragg gratings, IEEE Photon. Technol. Lett. **24**(15), 1319–1321 (2012).

[131] Y. Wang, H. Chi, X. Zhang, S. Zheng, and X. Jin, Photonic approach for microwave spectral analysis based on Fourier cosine transform, Opt. Lett. **36**(19), 3897–3899 (2011).

[132] E. J. Candés and M. B. Wakin, An introduction to compressive sampling, IEEE Signal Proc. Mag. **25**(2), 21–30 (2008).

[133] J. Nichols and F. Bucholtz, Beating Nyquist with light: a compressively sampled photonic link, Opt. Express **19**(8), 7339–7348 (2011).

[134] H. Nan, Y. Gu, and H. Zhang, Optical analog-to-digital conversion system based on compressive sampling, IEEE Photon. Technol. Lett. **23**(2), 67–69 (2011).

[135] H. Chi, Y. Mei, Y. Chen, D. Wang, S. Zheng, X. Jin, and X. Zhang, Microwave spectral analysis based on photonic compressive sampling with random demodulation, Opt. Lett. **37**(22), 4636–4638 (2012).

[136] G. C. Valley, G. A. Sefler, and T. J. Shaw, Compressive sensing of sparse radio frequency signals using optical mixing, Opt. Lett. **37**(22), 4675–4677 (2012).

[137] Y. Liang, M. Chen, H. Chen, C. Lei, P. Li, and S. Xie, Photonic-assisted multi-channel compressive sampling based on effective time delay pattern, Opt. Express **21**(22), 25700–25707 (2013).

[138] H. Chi, Y. Chen, Y. Mei, X. Jin, S. Zheng, and X. Zhang, Microwave spectrum sensing based on photonic time stretch and compressive sampling, Opt. Lett. **38**(2), 136–138 (2013).

[139] Y. Chen, H. Chi, T. Jin, S. Zheng, X. Jin, and X. Zhang, Sub-Nyquist sampled analog-to-digital conversion based on photonic time stretch and compressive sensing with

optical random mixing, J. Lightwave Technol. **31**(21), 3395–3401 (2013).

[140] F. F. Yin, Y. Y. Gao, Y. T. Dai, J. Y. Zhang, K. Xu, Z P. Zhang, J Q. Li, and J T. Lin, Multifrequency radio frequency sensing with photonics-assisted spectrum compression, Opt. Lett. **38**(21), 4386–4388 (2013).

[141] Y. Chen, X. Yu, H. Chi, H. Jin, X. Zhang, S. Zheng, and M. Galili, Compressive sensing in a photonic link with optical integration, Opt. Lett. **39**(8), 2222–2224 (2014).

[142] Q. Guo, Y. Liang, M. Chen, H. Chen, and S. Xie, Compressive spectrum sensing of radar pulses based on photonic techniques, Opt. Express **23**(4), 4517–4522 (2015).

[143] T. P. McKenna, J. H. Kalkavage, M. D. Sharp, and T. R. Clark, Wideband photonic compressive sampling system, J. Lightwave Technol. **34**(11), 2484–2855 (2016).

[144] E. Salik, N. Yu, L. Maleki, and E. Rubiola, Dual photonic-delay line cross correlation method for phase-noise measurement, IEEE International Frequency Control Symposium and Exposition, 303–306, 2004.

[145] E. Rubiola, E. Salik, S. Huang, N. Yu, and L. Maleki, Photonic-delay technique for phase-noise measurement of microwave oscillators, J. Opt. Soc. Am. B. **22**(5), 987–997 (2005).

[146] P. Salzenstein, J. Cussey, X. Jouvenceau, H. Tavernier, L. Larger, E. Rubiola, and G. Sauvage, Realization of a phase-noise measurement bench using cross correlation and double optical delay line, Acta Phys. Pol. A. **112**(5), 1107 (2007).

[147] D. Zhu, F. Zhang, P. Zhou, D. Zhu, and S. Pan, Wideband phase-noise measurement using a multifunctional microwave photonic processor, IEEE Photon. Technol. Lett. **26**(24), 2434–2437 (2014).

[148] D. Zhu, F. Zhang, P. Zhou, and S. Pan, Phase-noise measurement of wideband microwave sources based on a microwave photonic frequency downconverter, Opt. Lett. **40**(7), 1326–1329 (2015).

[149] F. Scotti, F. Laghezza, P. Ghelfi, and A. Bogoni, Multiband software-defined coherent radar based on a single photonic transceiver, IEEE Trans. Microw. Theory Techn. **63**(2), 546–552 (2015).

[150] P. Ghelfi, F. Laghezza, F. Scotti, D. Onori, and A. Bogoni, Photonics for radars operating on multiple coherent bands, J. Lightwave Technol. **34**(2), 500–507 (2016).

[151] F. Scotti, D. Onori, M. Scaffardi, E. Lazzeri, A. Bogoni, and F. Laghezza, Multi-frequency lidar/radar integrated system for robust and flexible Doppler measurements, IEEE Photon. Technol. Lett. **27**(21), 2268–2271 (2015).

[152] V. Vercesi, D. Onori, F. Laghezza, F. Scotti, A. Bogoni, and M. Scaffardi, Frequency-agile dual-frequency lidar for integrated coherent radar-lidar architectures, Opt. Lett. **40**(7), 1358–1361 (2015).

[153] Photonic coherent 250 GHz sensor, https://idw-online.de/de/news638903; https://www.oe.uni-due.de/start/forschung/projekte/151006_photonic_sensor_uar.asp?l=de, accessed: Dec. 2015.

[154] J. Capmany, G. Li, C. Lim, and J. Yao, Microwave photonics: current challenges towards widespread application, Opt. Express **21**(19), 22862–22867 (2013).

[155] L. Coldren, S. C. Nicholes, L. Johansson, S. Ristic, R. S. Guzzon, E. J. Norberg, and U. Krishnamachari, High per-

[156] M. J. Heck, J. F. Bauters, M. L. Davenport, D. T. Spencer, and J. E. Bowers, Ultra-low loss waveguide platform and its integration with silicon photonics, Laser Photon. Rev. **8**(5), 667–686 (2014).

[157] M. Heck, J. F. Bauters, M. L. Davenport, J. K. Doylend, S. Jain, G. Kurczveil, S. Srinivasan, Y. Tang, and J. E. Bowers, Hybrid silicon photonic integrated circuit technology, IEEE J. Sel. Top. Quantum Electron. **19**(4), 6100117 (2013).

[158] P. Dong, N.-N. Feng, D. Feng, W. Qian, H. Liang, D. C. Lee, B. Luff, T. Banwell, A. Agarwal, P. Toliver, R. Menendez, T. K. Woodward, and M. Asghari, GHz-bandwidth optical filters based on high-order silicon ring resonators, Opt. Express **18**(23), 23784–23789 (2010).

[159] J. Lloret, J. Sancho, M. Pu, I. Gasulla, K. Yvind, S. Sales, and J. Capmany, Tunable complex-valued multi-tap microwave photonic filter based on single silicon-on-insulator microring resonator, Opt. Express **19**(13), 12402–12407 (2011).

[160] D. Marpaung, B. Morrison, M. Pagani, R. Pant, D. Y. Choi, B. Luther-Davies, S. J. Madden, and B. J. Eggleton, Low-power, chip-based stimulated Brillouin scattering microwave photonic filter with ultrahigh selectivity, Optica **2**(2), 76–83 (2015).

[161] L. Zhuang, C. G. Roeloffzen, A. Meijerink, M. Burla, D. A. Marpaung, A. Leinse, M. Hoekman, R. G. Heideman, and W. Van Etten, Novel ring resonator-based integrated photonic beamformer for broadband phased array receive antennas part II: experimental prototype, J. Lightwave Technol. **28**(1), 19–31 (2010).

[162] R. Pant, D. Marpaung, I. V. Kabakova, B. Morrison, C. G. Poulton, and B. J. Eggleton, On-chip stimulated Brillouin scattering for microwave signal processing and generation, Laser Photon. Rev. **8**(5), 653–666 (2014).

[163] A. El Nagdi, K. Liu, T. P. LaFave, L. R. Hunt, V. Ramakrishna, M. Dabkowski, D. L. MacFarlane, and M. P. Christensen, Active integrated filters for RF-photonic channelizers, Sensors **11**(2), 1297–1320 (2011).

[164] E. Buracchini, The software radio concept, IEEE Commun. Mag. **38**(9), 138–143 (2000).

[165] E. J. Norberg, R. S. Guzzon, J. S. Parker, L. A. Johansson, and L. A. Coldren, Programmable photonic microwave filters monolithically integrated in InP–InGaAsP, J. Lightwave Technol. **29**(11), 1611–1619 (2011).

[166] D. Onori, F. Laghezza, P. Ghelfi, S. Pinna, F. Scotti, G. Serafino, and A. Bogoni, Photonic ultra-wideband software-defined RF receiver for electronic spectrum measurements, Optical Fiber Communication Conference (OFC), paper.Th4H-3, 2014.

[167] J. Wang, H. Yu, M. Chen, H. Chen, S. Yang, and S. Xie, Large frequency range photonic-assisted software-defined radio transceiver, Conference on Lasers and Electro-Optics (CLEO), paper.STh4F-8, 2015.

[168] P. Ghelfi, F. Laghezza, F. Scotti, G. Serafino, S. Pinna, and A. Bogoni, Photonic generation and independent steering of multiple RF signals for software defined radars, Opt. Express **21**(19), 22905–22910 (2013).

[169] F. Scotti, F. Laghezza, G. Serafino, S. Pinna, D. Onori, P. Ghelfi, and A. Bogoni, In-field experiments of the first photonics-based software-defined coherent radar, J. Lightwave Technol. **32**(20), 3365–3372 (2014).

[170] P. Ghelfi, F. Laghezza, F. Scotti, G. Serafino, S. Pinna, D. Onori, E. Lazzeri, and A. Bogoni, Photonics in radar systems: RF integration for state-of-the-art functionality, IEEE Microw. Mag. **16**(8), 74–83 (2015).

[171] S. Pan, D. Zhu, S. Liu, K. Xu, Y. Dai, T. Wang, J. Liu, N. Zhu, Y. Xue, and N. Liu, Satellite payloads pay off, IEEE Microw Mag. **16**(8), 61–73 (2015).

[172] D. Perez, I. Gasulla, and J. Capmany, Software-defined reconfigurable microwave photonics processor, Opt. Express **23**(11), 14640–14654 (2015).

[173] L. Zhuang, C. G. H. Roeloffzen, M. Hoekman, K. J. Boller, and A. J. Lowery, Programmable photonic signal processor chip for radiofrequency applications, Optica, **2**(10), 854–859 (2015).

[174] W. Liu, M. Li, R. S. Guzzon, E. J. Norberg, J. S. Parker, M. Lu, L. A. Coldren, and J. Yao, A fully reconfigurable photonic integrated signal processor, Nature Photon. **10**(3), 190–196 (2016).